



May 30<sup>th</sup> 2008 – X-ray Universe 2008 – Granada, Spain

# Spectral Energy Distribution of Hyper-Luminous Infrared Galaxies

Ángel Ruiz<sup>1</sup>

Francisco J. Carrera<sup>1</sup>, Francesca Panessa<sup>2</sup>, Giovanni Miniutti<sup>3</sup>

1: Instituto de Física de Cantabria (CSIC-UC)

2: INAF/IASF – Roma

3: Laboratoire APC - Paris





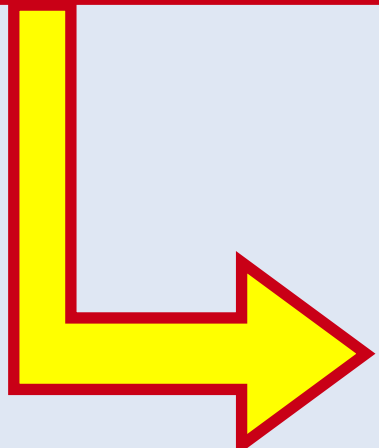
# What is all the fuss about?

- Supermassive Black Holes in centers of most local galaxies ([Kormendy & Gebhardt, 2001](#))
- Correlation between mass of central BH and spheroid ([Magorrian et al. 1998; McLure & Dunlop, 2002](#))
- Similar evolution of X-ray AGN and optical galaxies ([Silvermann et al. 2005](#))



# What is all the fuss about?

- Supermassive Black Holes in centers of most local galaxies (Kormendy & Gebhardt, 2001)
- Correlation between mass of central BH and spheroid (Magorrian et al. 1998; McLure & Dunlop 2002)
- Similar evolution of X-ray AGN and optical galaxies (Silvermann et al. 2005)



**Connected growth of central BH through accretion and spheroid through star formation**



# AGN-galaxy co-evolution

- **Strong evidence of AGN-galaxy co-evolution:**
  - Connection between the growth of central SMBH through **accretion** and spheroid through **star formation**
- **How to observe AGN-galaxy coeval:**
  - **Star formation** takes place in heavily obscured environments: need penetrating radiation:
    - **X-rays** (of course!): thermal bremsstrahlung, binaries
    - **MIR-FIR-submm**: radiation absorbed and re-emitted
    - Radio
  - SMBH growth through accretion produces **AGN activity**:
    - **X-rays** are the "smoking gun", **but**:
      - Most accretion power in the Universe absorbed (**Fabian & Iwasawa 1999**)
      - X-ray background synthesis model require most AGN in the Universe absorbed (**Gilli et al. 1999**)
    - "Warm" **MIR-FIR** colours: direct emission absorbed and re-emitted
    - Radio



# AGN-galaxy co-evolution

- Strong evidence of AGN-galaxy co-evolution:
  - Connection between the growth of central SMBH through **accretion** and spheroid through **star formation**
- How to observe AGN-galaxy coeval:
  - **Happy marriage of X-ray and MIR-FIR astronomy: coincidence in time of Chandra, XMM-Newton, Suzaku, Spitzer, Akari, Herschel...**
  - Radio
- SMBH growth through accretion produces **AGN activity**:
  - **X-rays** are the "smoking gun", **but**:
    - Most accretion power in the Universe absorbed (**Fabian & Iwasawa 1999**)
    - X-ray background synthesis model require most AGN in the Universe absorbed (**Gilli et al. 1999**)
  - "Warm" **MIR-FIR** colours: direct emission absorbed and re-emitted
  - Radio

# Observing AGN-galaxy co-evolution in X-rays and MIR-FIR



- **Multi-wavelength surveys: AEGIS, GOODS, COSMOS**  
*(see Brusa's talk)*
- **Targeted MIR observations of X-ray sources:**
  - X-ray absorbed broad line QSO *(see Page's talk)*
- **Targeted X-ray observations of MIR-FIR-emitting objects:**
  - Ultraluminous IR Galaxies  
*(Franceschini et al. 2003, Teng et al. 2005,  
Poster G-1 by Anabuki)*
  - **Hyperluminous IR Galaxies**  
*(this talk, Ruiz et al. 2007)*



# Why HLIRGs?

- $L_{8-1000\mu\text{m}} = 10^{12}\text{-}10^{13} L_{\text{sol}}$ : **ULIRGS**
  - Powered by starburst (STB) and some ( $\sim 50\%$ ) harbour AGN ([Farrah et al. 2003](#))
  - Fraction of AGN increases with IR luminosity ([Veilleux et al. 1999](#))
  - Most in interacting systems ([Farrah et al. 2001](#))
  - Sample in X-rays: composite, STB dominated ([Franceschini et al. 2003; Teng et al. 2005](#))
- $L_{8-1000\mu\text{m}} > 10^{13} L_{\text{sol}}$ : **HLIRGS** ([Rowan-Robinson 2000 \[RR00\]](#))
  - Most with AGN contribution ([RR00, Farrah et al. 2002a](#))
  - Only some interacting ( $\sim 30\%$ ) ([Farrah et al. 2002b](#))
    - ***Not trivially high luminosity tail of ULIRGs***
  - Some present heavy obscuration in X-rays, even Compton-Thick ([Wilman et al. 2003, Iwasawa et al. 2005; Nandra et al. 2007](#))



# Why HLIRGs?

- $L_{8-1000\mu m} = 10^{12}-10^{13} L_{sol}$ : ULIRGS
  - Powered by starburst (STB) and some (~50%) harbour AGN (Wilman et al. 2003)
- HLIRGs:
  - Strong star formation:  $> 1000 M_{\odot} / \text{yr}$
  - High AGN fraction
- Good laboratory to investigate star formation and BH growth:
  - Young galaxies experiencing burst of star formation?
  - Transient phase in AGN evolution?
  - ....
- *Not trivially high luminosity tail of ULIRGs*
  - Some present heavy obscuration in X-rays, even Compton-Thick (Wilman et al. 2003, Iwasawa et al. 2005; Nandra et al. 2007)

# An XMM-Newton study of HLIRGs: Sample



- Out of the 45 **RR00 sample**, those with:
  - Public XMM-Newton data as of Dec. 2004
  - Own XMM-Newton AO-5 data
  - $z < \sim 2$ : avoid strong biasing due to high  $z$  QSOs
- 14 objects in final sample:
  - All SED fitting in MIR/FIR  
**(RR00, Farrah et al. 2002, Verma et al. 2002)**

|     | <b>Source</b>    | <b>Type<br/>(opt)</b> | <b>z</b> | <b>AGN / STB<br/>(IR SED fitting)</b> | <b>CT?</b> |
|-----|------------------|-----------------------|----------|---------------------------------------|------------|
| 248 | IRAS F00235+1024 | Starburst             | 0.575    | 0.5/0.5                               | ✓          |
|     | IRAS 07380-2342  | Starburst             | 0.292    | 0.6/0.4                               | X          |
|     | IRAS 00182-7112  | QSO 2                 | 0.327    | 0.35/0.65                             | ✓          |
|     | IRAS 09104+4109  | QSO 2                 | 0.442    | 1/0                                   | ✓          |
|     | IRAS 12514+1027  | Seyfert 2             | 0.3      | 0.4/0.6                               | ✓          |
|     | IRAS F15307+3252 | Seyfert 2             | 0.926    | 0.7/0.3                               | ✓          |
|     | PG 1206+459      | QSO                   | 1.158    | 1/0                                   | X          |
|     | PG 1247+267      | QSO                   | 2.038    | 1/0                                   | X          |
|     | IRAS F12509+3122 | QSO                   | 0.780    | 0.6/0.4                               | X          |
|     | IRAS 13279+3401  | QSO                   | 0.36     | 0.7/0.3                               | X          |
|     | IRAS 14026+4341  | QSO 1.5               | 0.323    | 0.6/0.4                               | X          |
|     | IRAS F14218+3845 | QSO                   | 1.21     | 0.2/0.8                               | X          |
|     | IRAS 16347+7037  | QSO                   | 1.334    | 0.8/0.2                               | X          |
|     | IRAS 18216+6418  | QSO                   | 0.297    | 0.6/0.4                               | X          |

# Not detected with XMM-Newton

| Source           | Model  | $\log L_{0.5-2}$ | $\log L_{2-10}$ | CT? |
|------------------|--|------------------|-----------------|-----|
| IRAS F00235+1024 | 3 $\sigma$ upper limit                         | -                | <42.4           | ✓   |
| IRAS 07380-2342  | 3 $\sigma$ upper limit                         | -                | <42.5           | X   |
| IRAS 00182-7112  | reflected+narrow line (0.8keV)                 | <41.9            | 44.8            | ✓   |
| IRAS 09104+4109  | “thermal”+reflected+narrow line                | 44.2             | 45.3            | ✓   |
| IRAS 12514+1027  | thermal+absorbed direct ( $4 \times 10^{23}$ ) | 42.2             | 43.3            | ✓   |
| IRAS F15307+3252 | “direct”                                       | <43.1            | 43.7–45.5       | ✓   |
| PG 1206+459      | direct   | <44.0            | 45.1            | X   |
| PG 1247+267      | “thermal”+direct                               | 45.5             | 45.9            | X   |
| IRAS F12509+3122 | “thermal”+direct                               | 43.8             | 44.3            | X   |
| IRAS 13279+3401  | 3 $\sigma$ upper limit                         | -                | <42.2           | X   |
| IRAS 14026+4341  | 3 $\sigma$ upper limit                         | -                | <42.6           | X   |
| IRAS F14218+3845 | direct   | <43.8            | 44.6            | X   |
| IRAS 16347+7037  | “thermal”+direct                               | 45.7             | 46.0            | X   |
| IRAS 18216+6418  | “thermal”+direct                               | 45.1             | 45.6            | X   |

# Strongly absorbed or no direct continuum

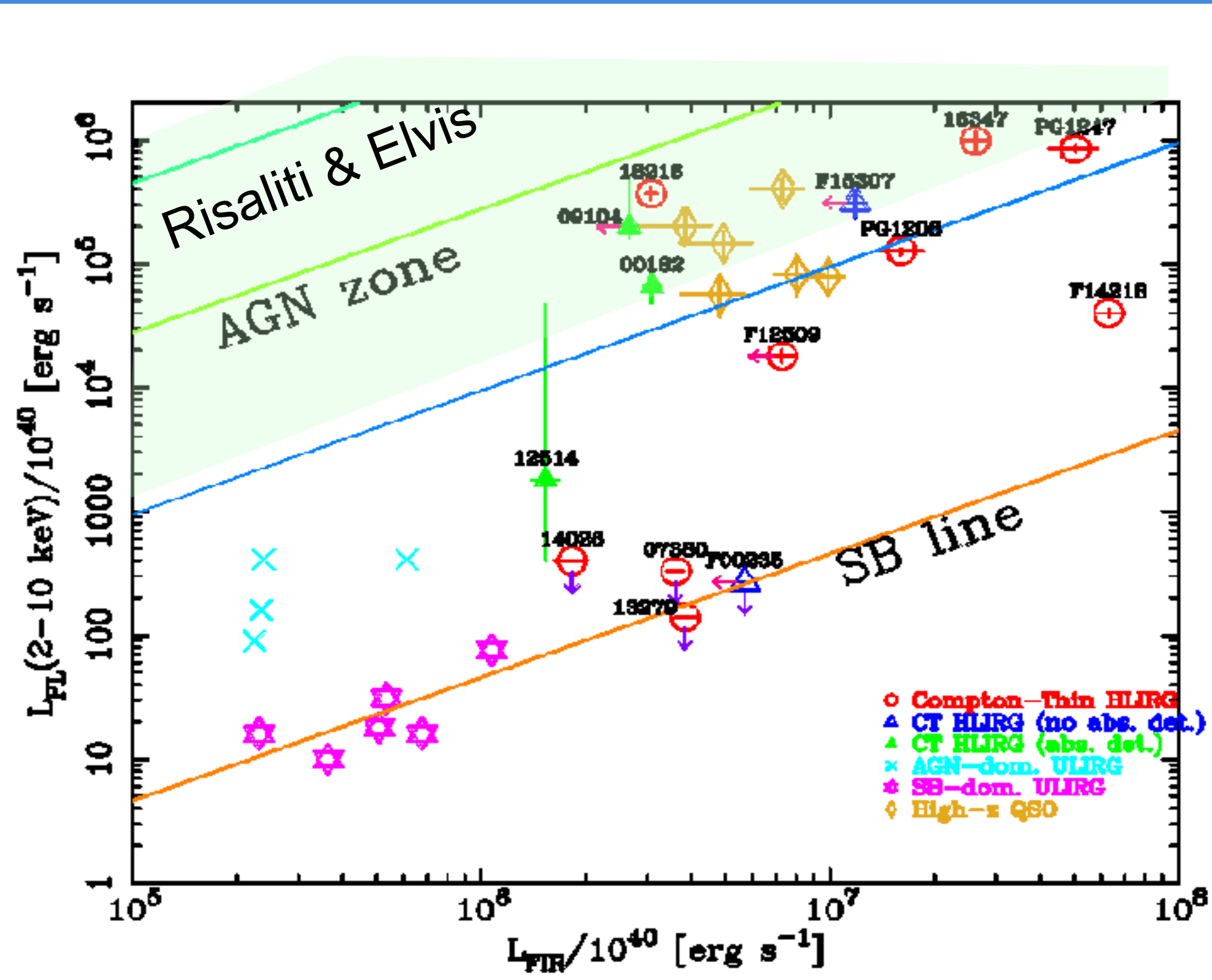
| Source           | Model  | $\log L_{0.5-2}$ | $\log L_{2-10}$ | CT? |
|------------------|--|------------------|-----------------|-----|
| IRAS F00235+1024 | $3\sigma$ upper limit                          | -                | <42.4           | ✓   |
| IRAS 07380-2342  | $3\sigma$ upper limit                          | -                | <42.5           | ✗   |
| IRAS 00182-7112  | reflected+narrow line (0.8keV)                 | <41.9            | 44.8            | ✓   |
| IRAS 09104+4109  | “thermal”+reflected+narrow line                | 44.2             | 45.3            | ✓   |
| IRAS 12514+1027  | thermal+absorbed direct ( $4 \times 10^{23}$ ) | 42.2             | 43.3            | ✓   |
| IRAS F15307+3252 | “direct”                                       | <43.1            | 43.7–45.5       | ✓   |
| PG 1206+459      | direct   | <44.0            | 45.1            | ✗   |
| PG 1247+267      | “thermal”+direct                               | 45.5             | 45.9            | ✗   |
| IRAS F12509+3122 | “thermal”+direct                               | 43.8             | 44.3            | ✗   |
| IRAS 13279+3401  | $3\sigma$ upper limit                          | -                | <42.2           | ✗   |
| IRAS 14026+4341  | $3\sigma$ upper limit                          | -                | <42.6           | ✗   |
| IRAS F14218+3845 | direct   | <43.8            | 44.6            | ✗   |
| IRAS 16347+7037  | “thermal”+direct                               | 45.7             | 46.0            | ✗   |
| IRAS 18216+6418  | “thermal”+direct                               | 45.1             | 45.6            | ✗   |

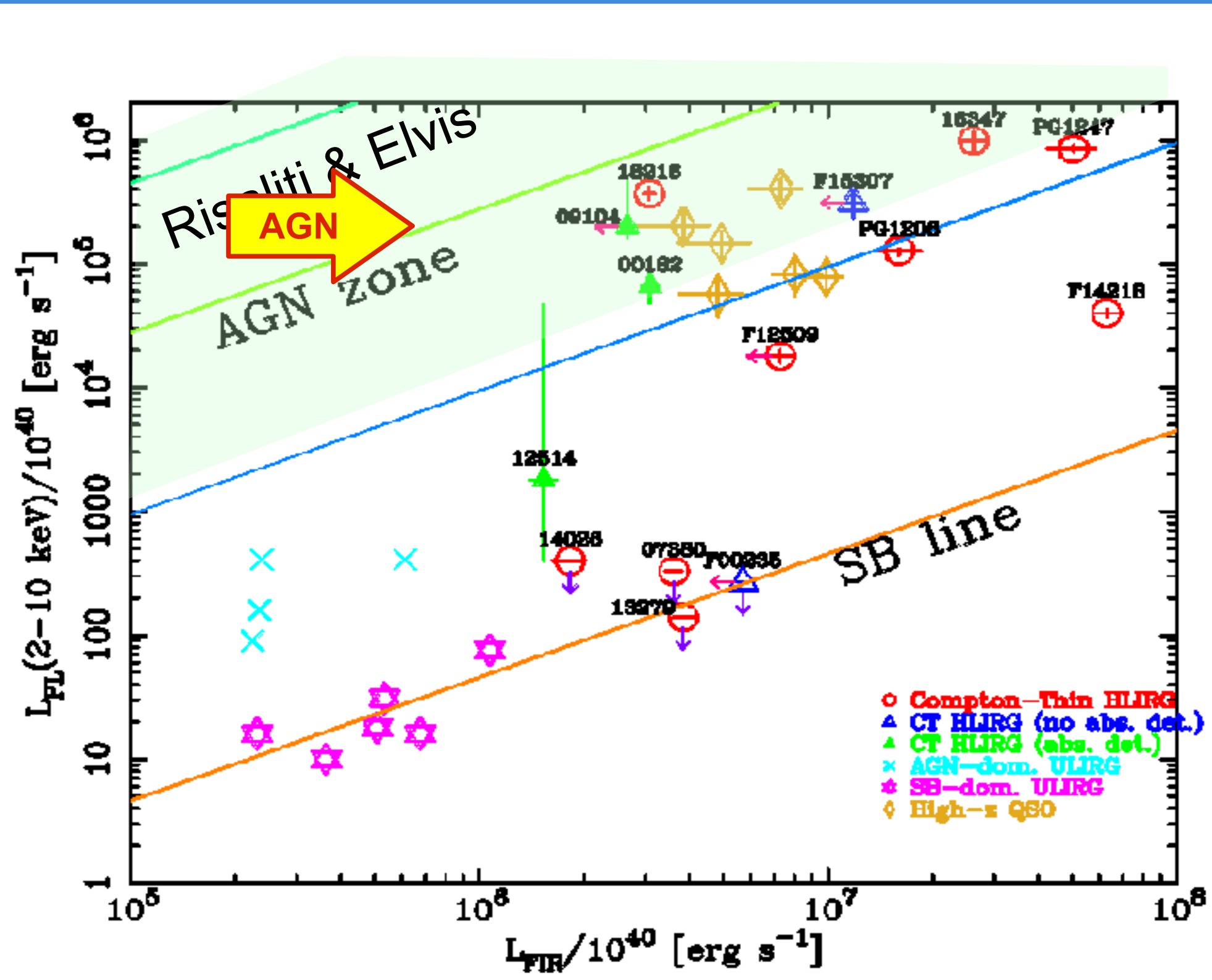
Soft excess: too bright to come from STB

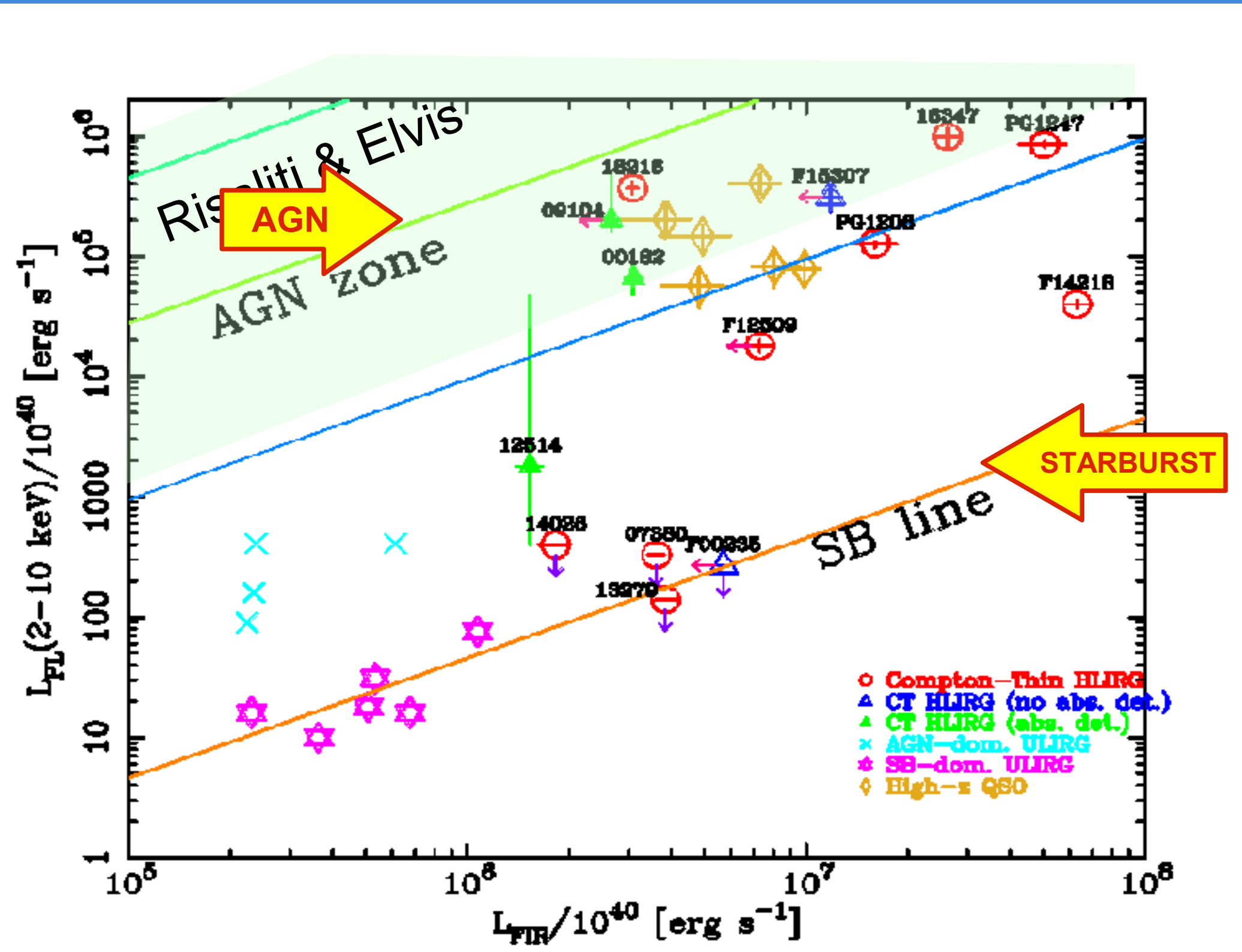
| Source           | Model  | $\log L_{0.5-2}$ | $\log L_{2-10}$ | CT? |
|------------------|--|------------------|-----------------|-----|
| IRAS F00235+1024 | $3\sigma$ upper limit                          | -                | <42.4           | ✓   |
| IRAS 07380-2342  | $3\sigma$ upper limit                          | -                | <42.5           | ✗   |
| IRAS 00182-7112  | reflected+narrow line (0.8keV)                 | <41.9            | 44.8            | ✓   |
| IRAS 09104+4109  | “thermal”+reflected+narrow line                | 44.2             | 45.3            | ✓   |
| IRAS 12514+1027  | thermal+absorbed direct ( $4 \times 10^{23}$ ) | 42.2             | 43.3            | ✓   |
| IRAS F15307+3252 | “direct”                                       | <43.1            | 43.7–45.5       | ✓   |
| PG 1206+459      | direct   | <44.0            | 45.1            | ✗   |
| PG 1247+267      | “thermal”+direct                               | 45.5             | 45.9            | ✗   |
| IRAS F12509+3122 | “thermal”+direct                               | 43.8             | 44.3            | ✗   |
| IRAS 13279+3401  | $3\sigma$ upper limit                          | -                | <42.2           | ✗   |
| IRAS 14026+4341  | $3\sigma$ upper limit                          | -                | <42.6           | ✗   |
| IRAS F14218+3845 | direct   | <43.8            | 44.6            | ✗   |
| IRAS 16347+7037  | “thermal”+direct                               | 45.7             | 46.0            | ✗   |
| IRAS 18216+6418  | “thermal”+direct                               | 45.1             | 45.6            | ✗   |

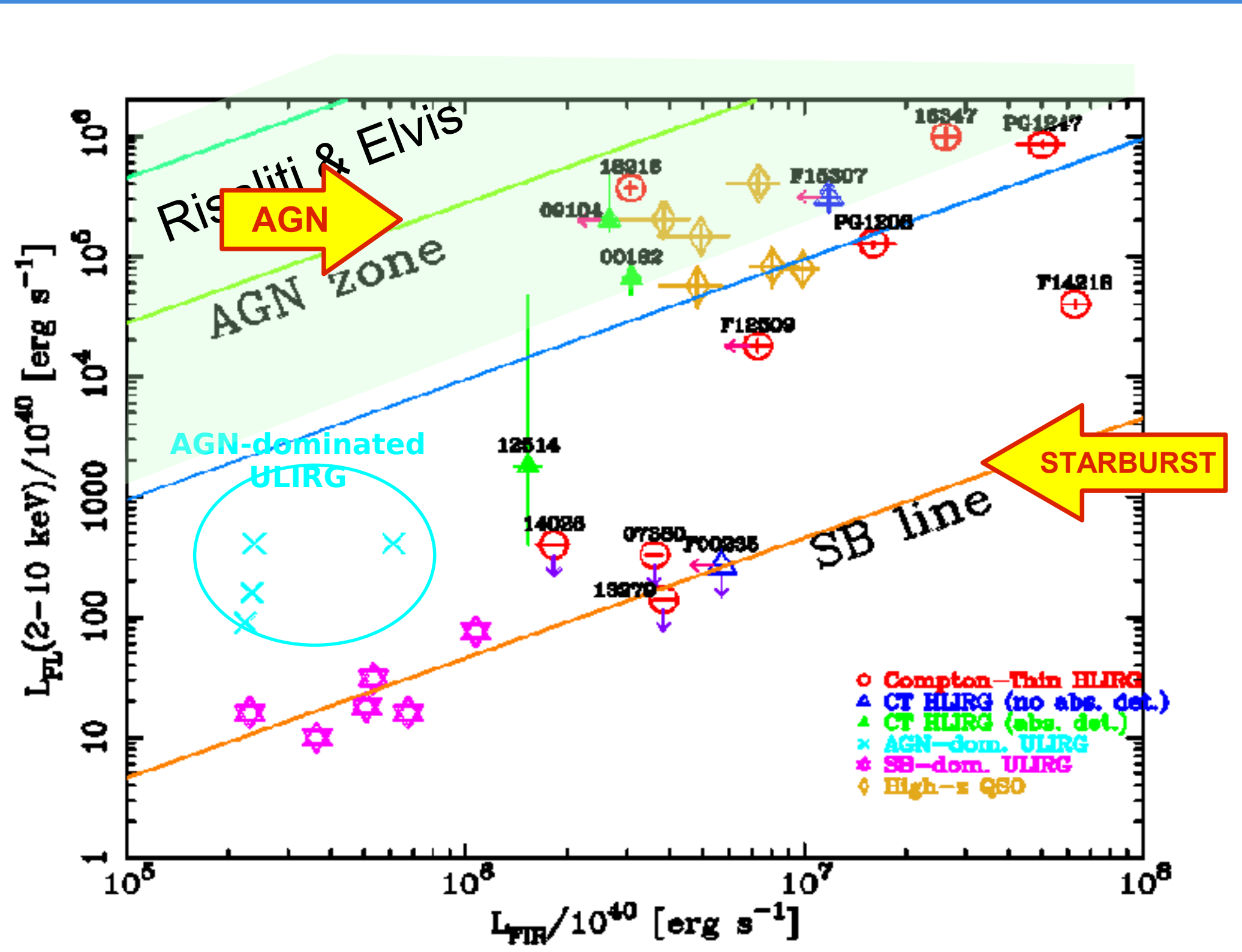
Only one detection of thermal emission from STB

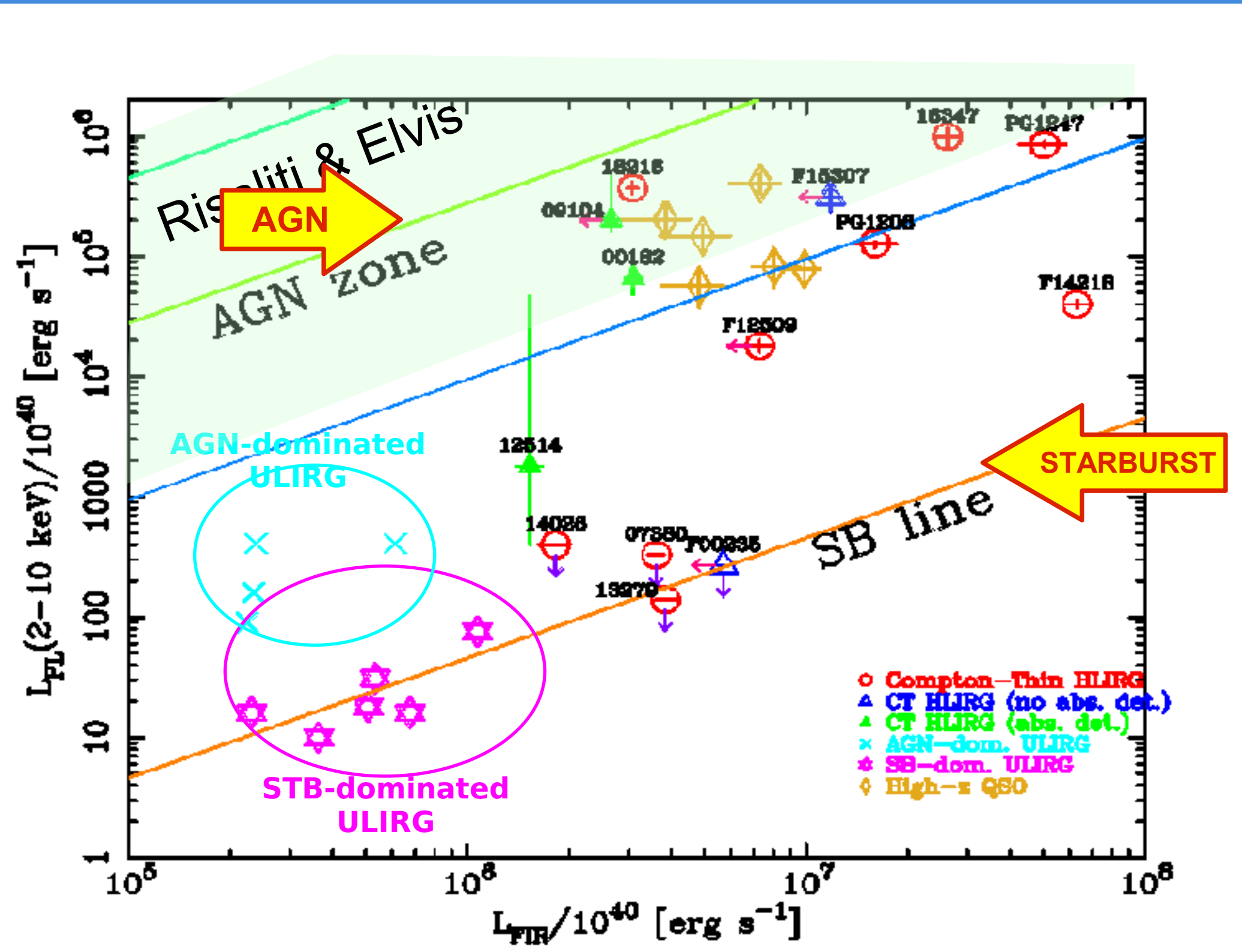
| Source           | Model  | $\log L_{0.5-2}$ | $\log L_{2-10}$ | CT? |
|------------------|--|------------------|-----------------|-----|
| IRAS F00235+1024 | $3\sigma$ upper limit                          | -                | <42.4           | ✓   |
| IRAS 07380-2342  | $3\sigma$ upper limit                          | -                | <42.5           | X   |
| IRAS 00182-7112  | reflected+narrow line (0.8keV)                 | <41.9            | 44.8            | ✓   |
| IRAS 09104+4109  | “thermal”+reflected+narrow line                | 44.2             | 45.3            | ✓   |
| IRAS 12514+1027  | thermal+absorbed direct ( $4 \times 10^{23}$ ) | 42.2             | 43.3            | ✓   |
| IRAS F15307+3252 | “direct”                                       | <43.1            | 43.7–45.5       | ✓   |
| PG 1206+459      | direct   | <44.0            | 45.1            | X   |
| PG 1247+267      | “thermal”+direct                               | 45.5             | 45.9            | X   |
| IRAS F12509+3122 | “thermal”+direct                               | 43.8             | 44.3            | X   |
| IRAS 13279+3401  | $3\sigma$ upper limit                          | -                | <42.2           | X   |
| IRAS 14026+4341  | $3\sigma$ upper limit                          | -                | <42.6           | X   |
| IRAS F14218+3845 | direct   | <43.8            | 44.6            | X   |
| IRAS 16347+7037  | “thermal”+direct                               | 45.7             | 46.0            | X   |
| IRAS 18216+6418  | “thermal”+direct                               | 45.1             | 45.6            | X   |

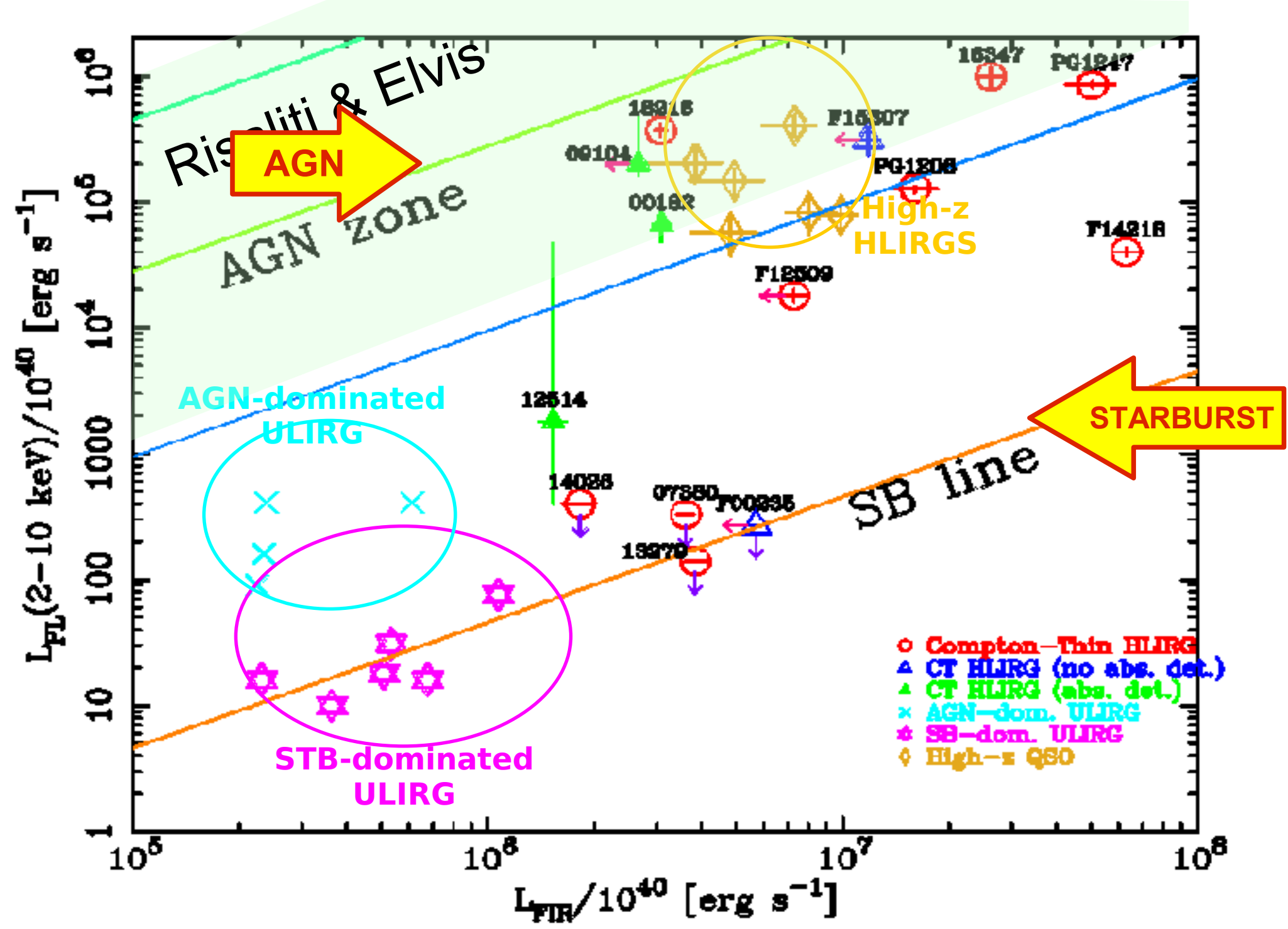


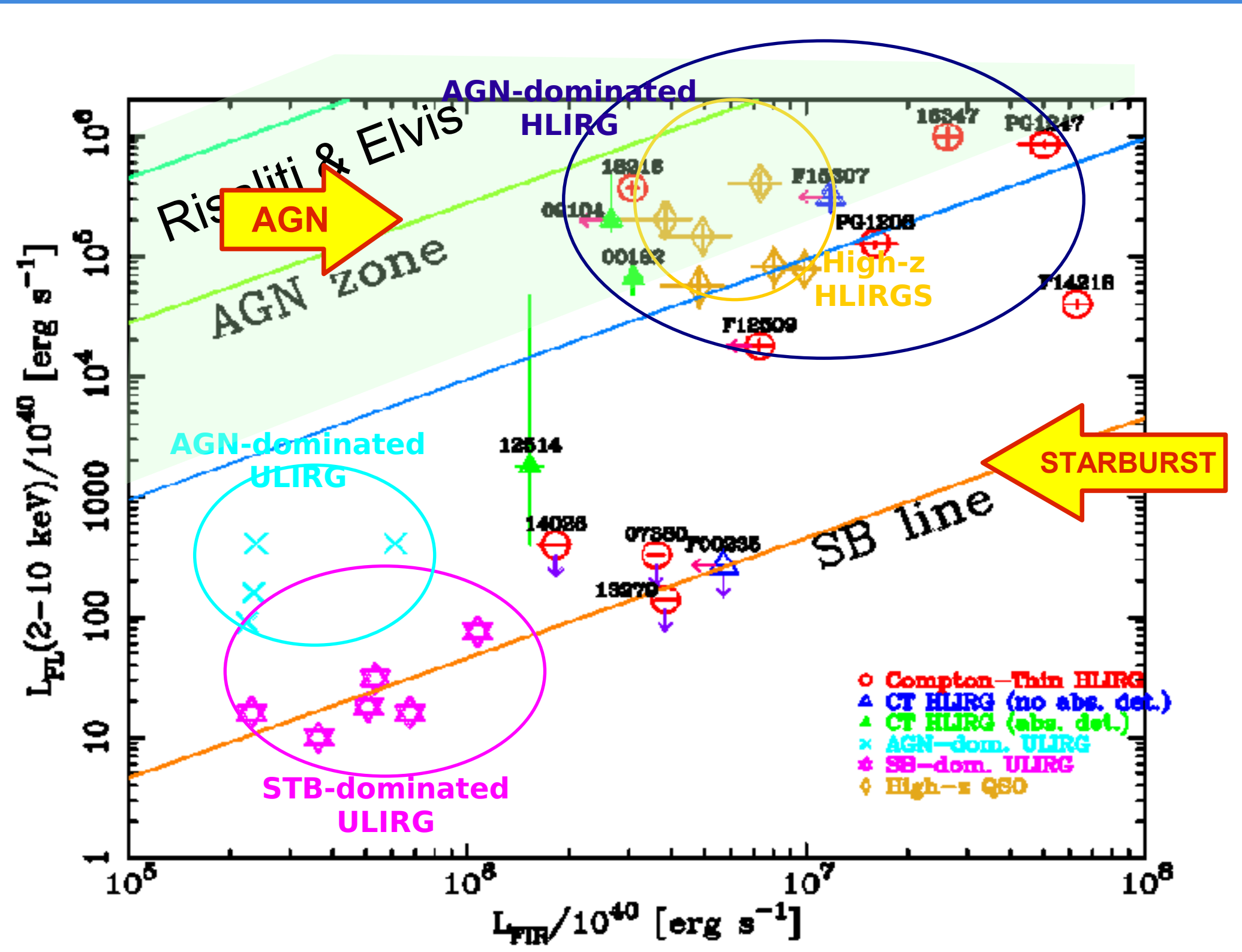


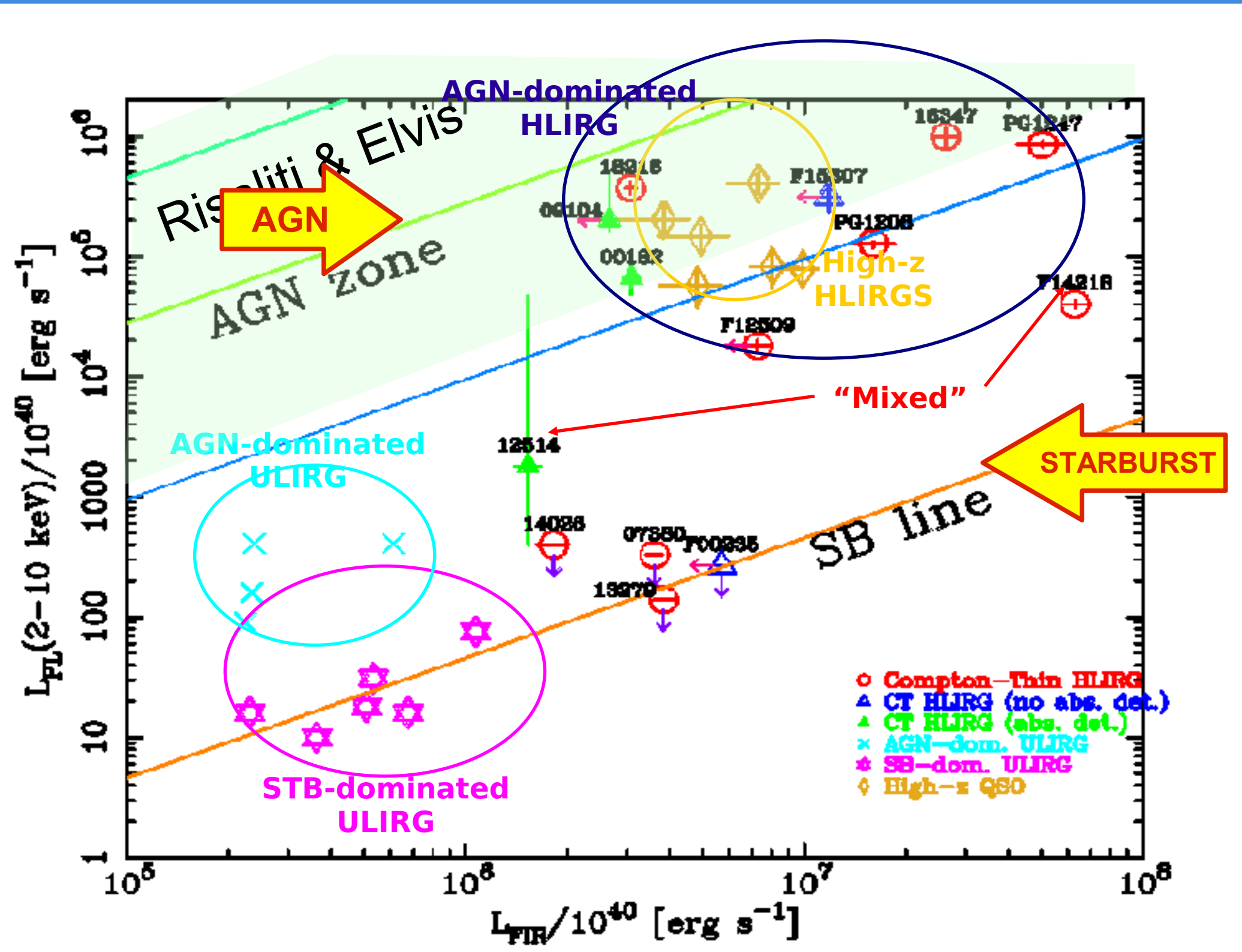


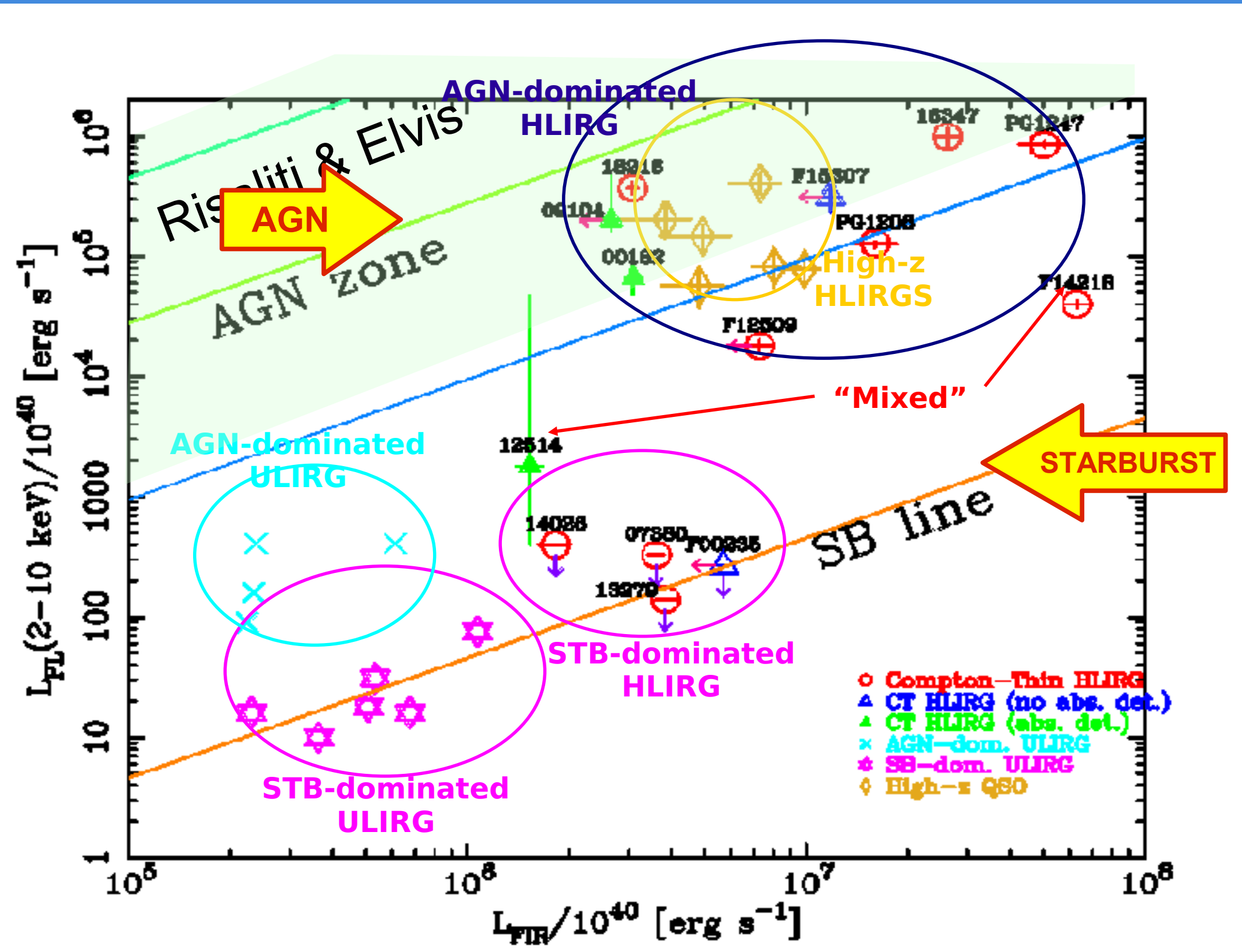


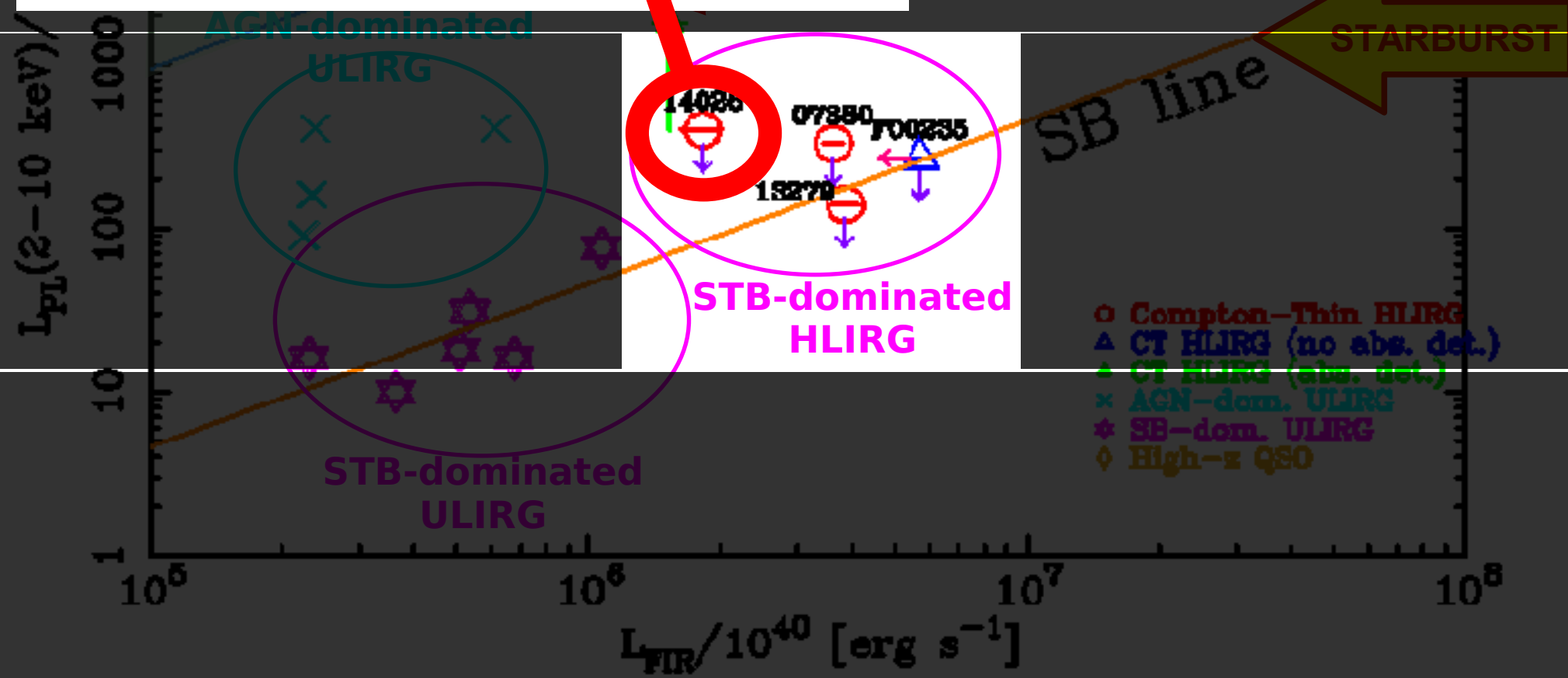
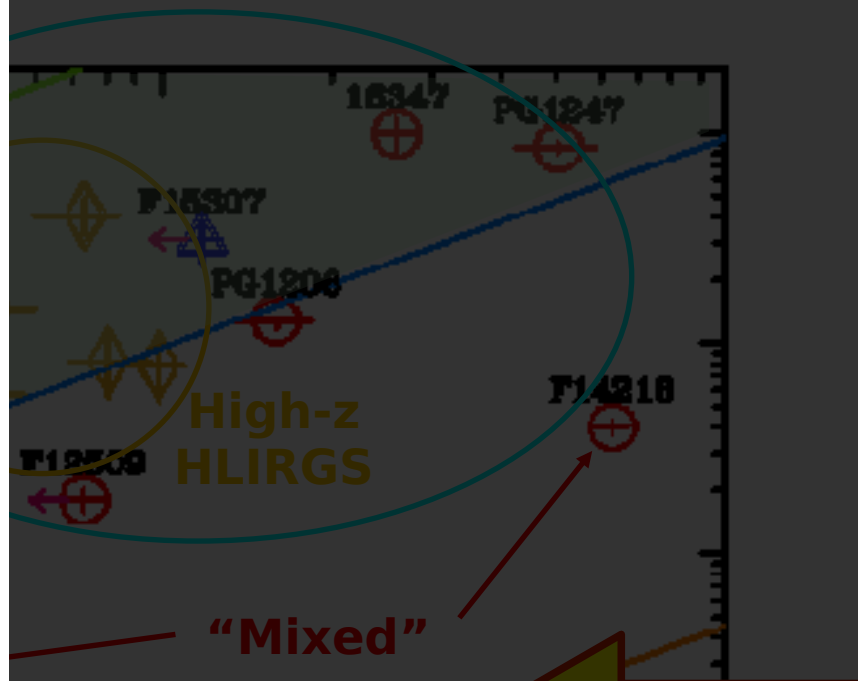
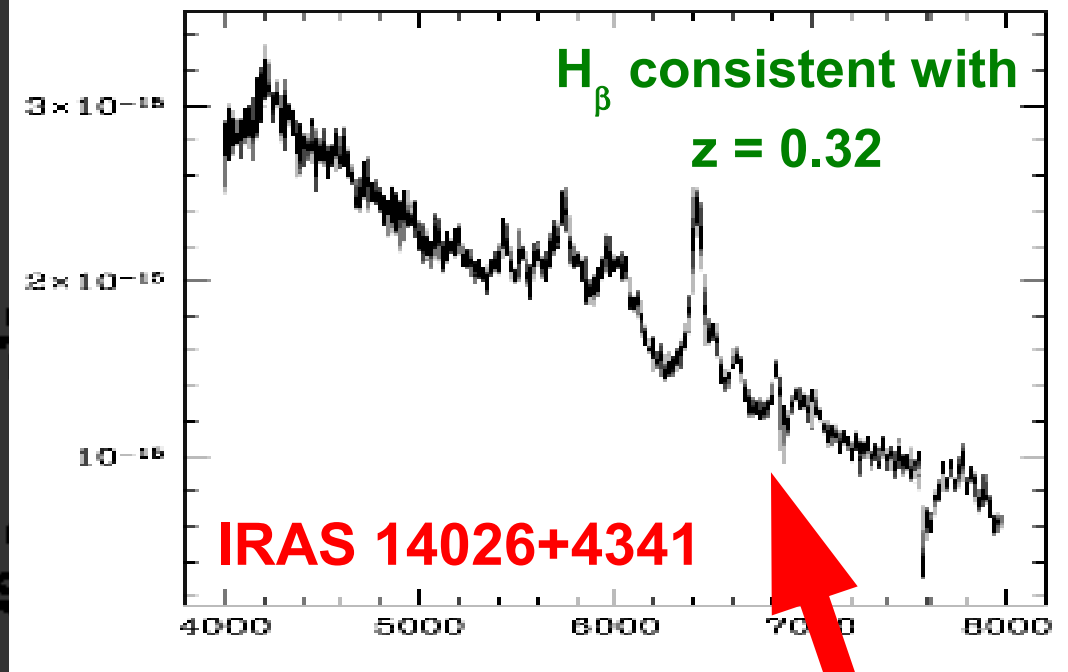


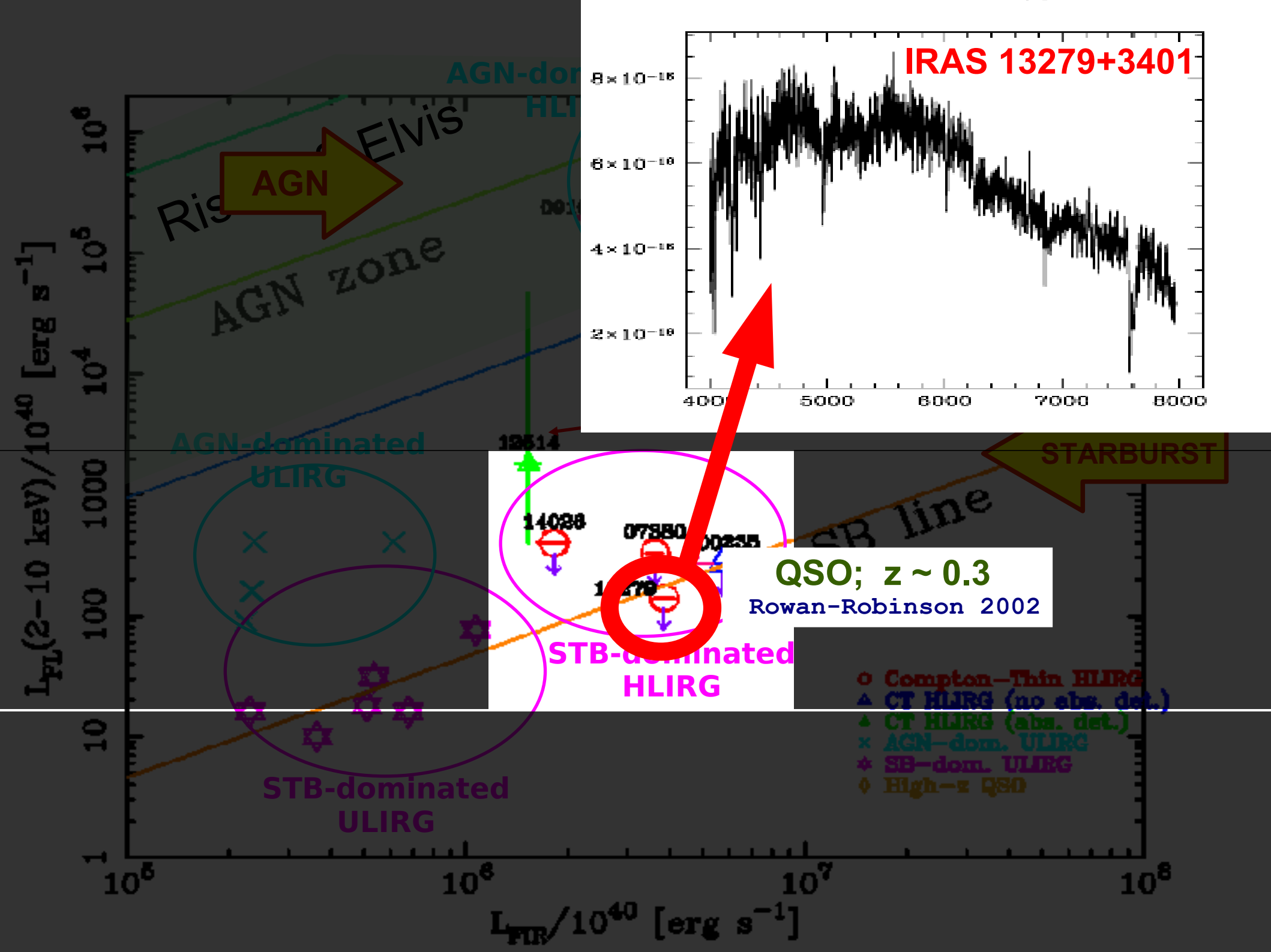


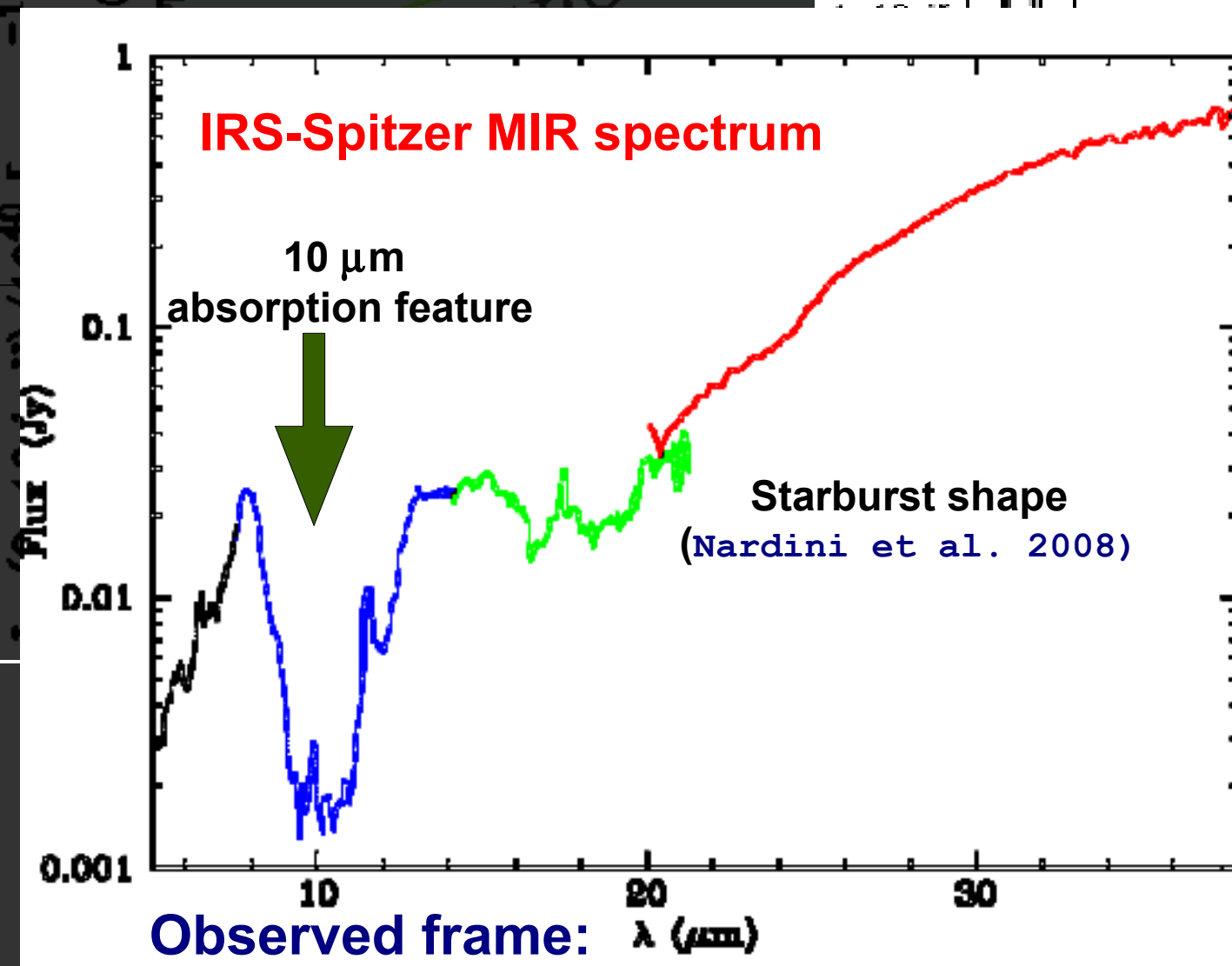
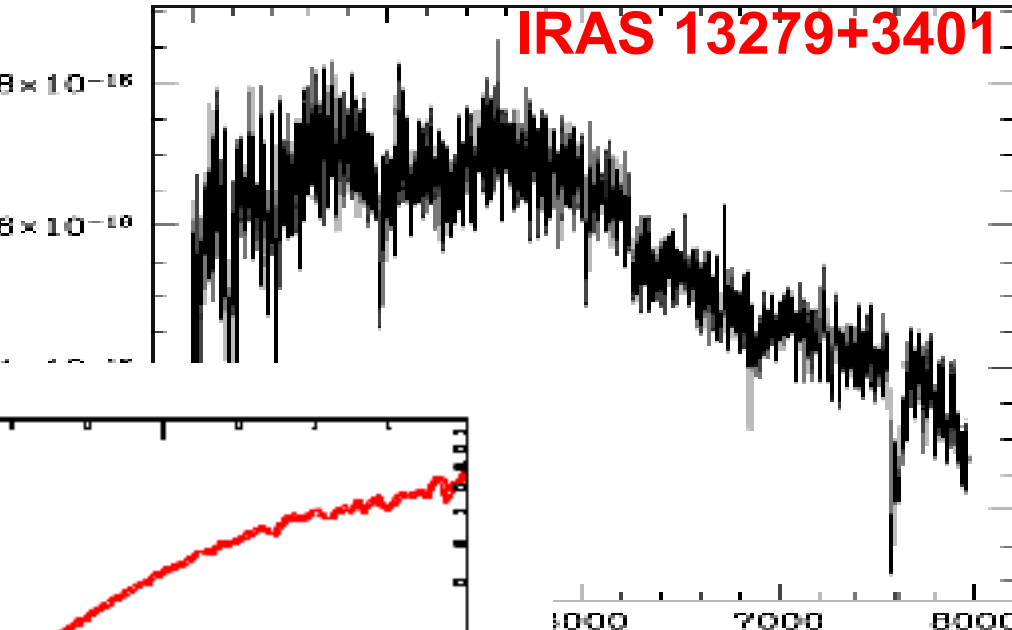


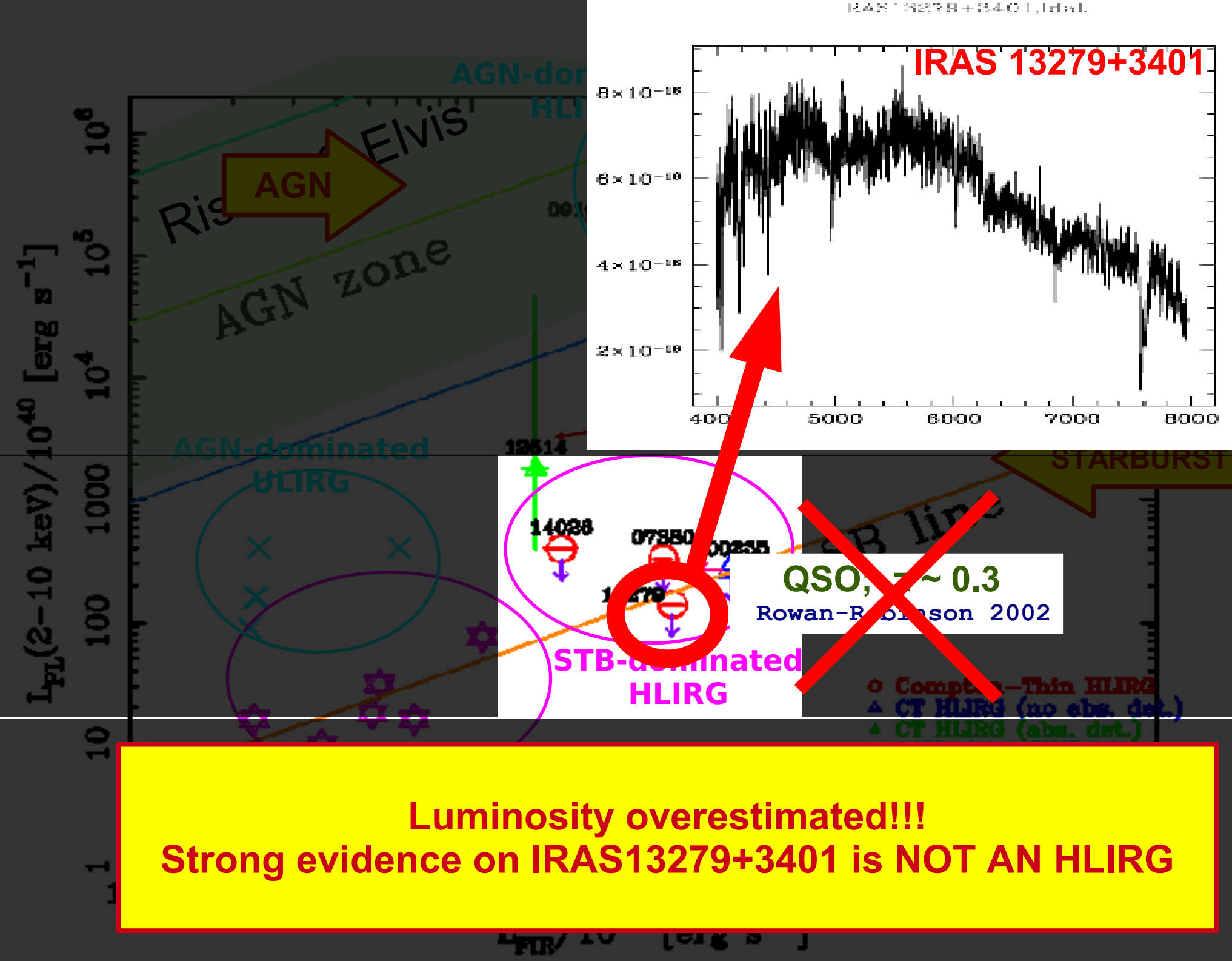


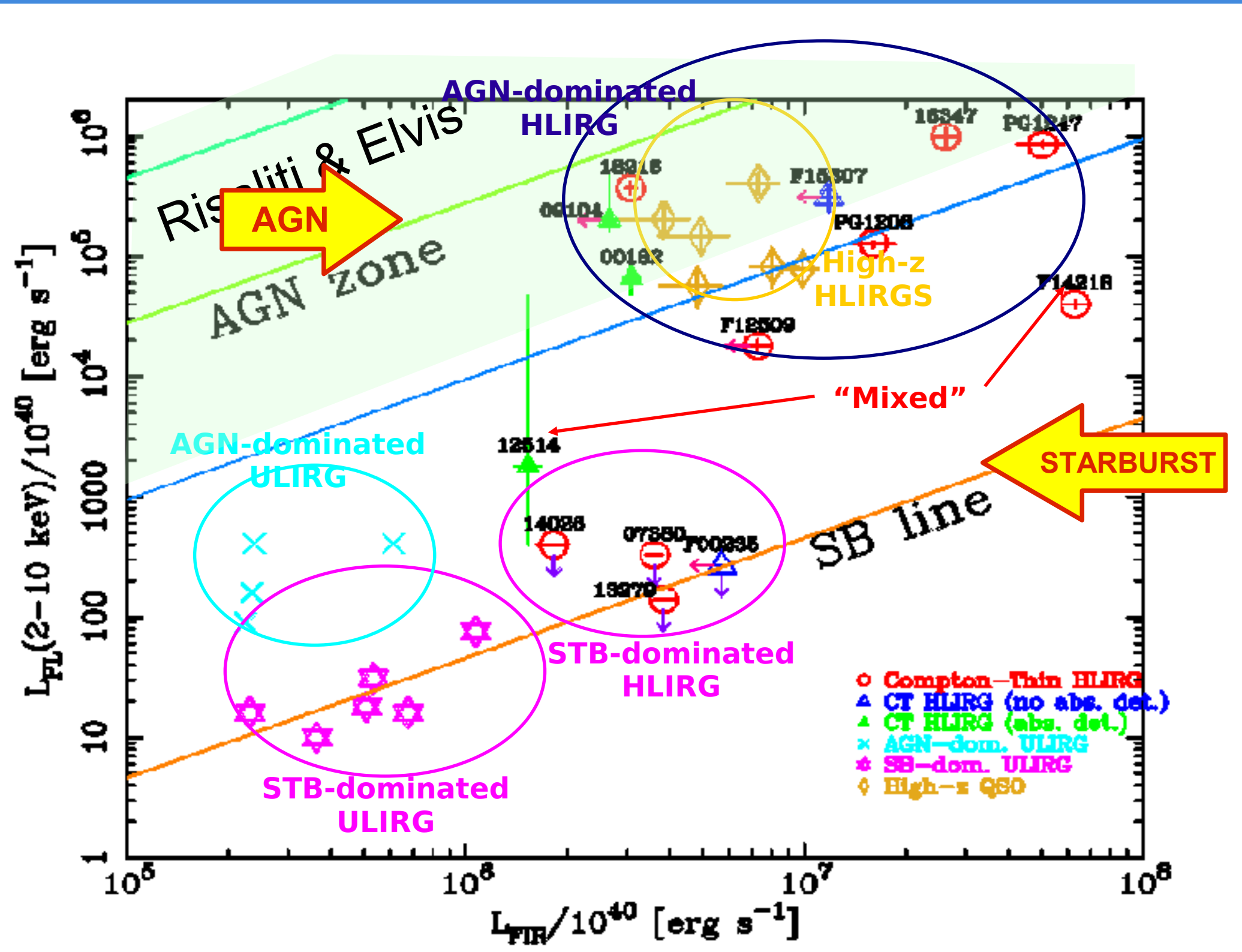












# Spectral Energy Distributions

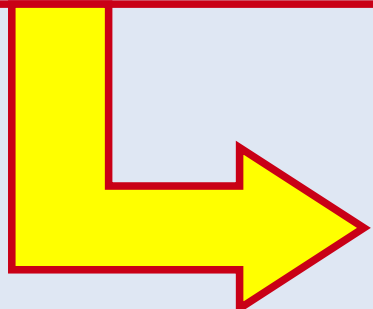


- Systematic IR excess (or underluminous in X-rays) with respect to local QSO SED:
  - X-ray obscuration?
  - Starburst excess?
  - Departure from standard local SED?
- STB and AGN relative contribution to the total output

# Spectral Energy Distributions



- Systematic IR excess (or underluminous in X-rays) with respect to local QSO SED:
  - X-ray obscuration?
  - Starburst excess?
  - Departure from standard local SED?
- STB and AGN relative contribution to the total output

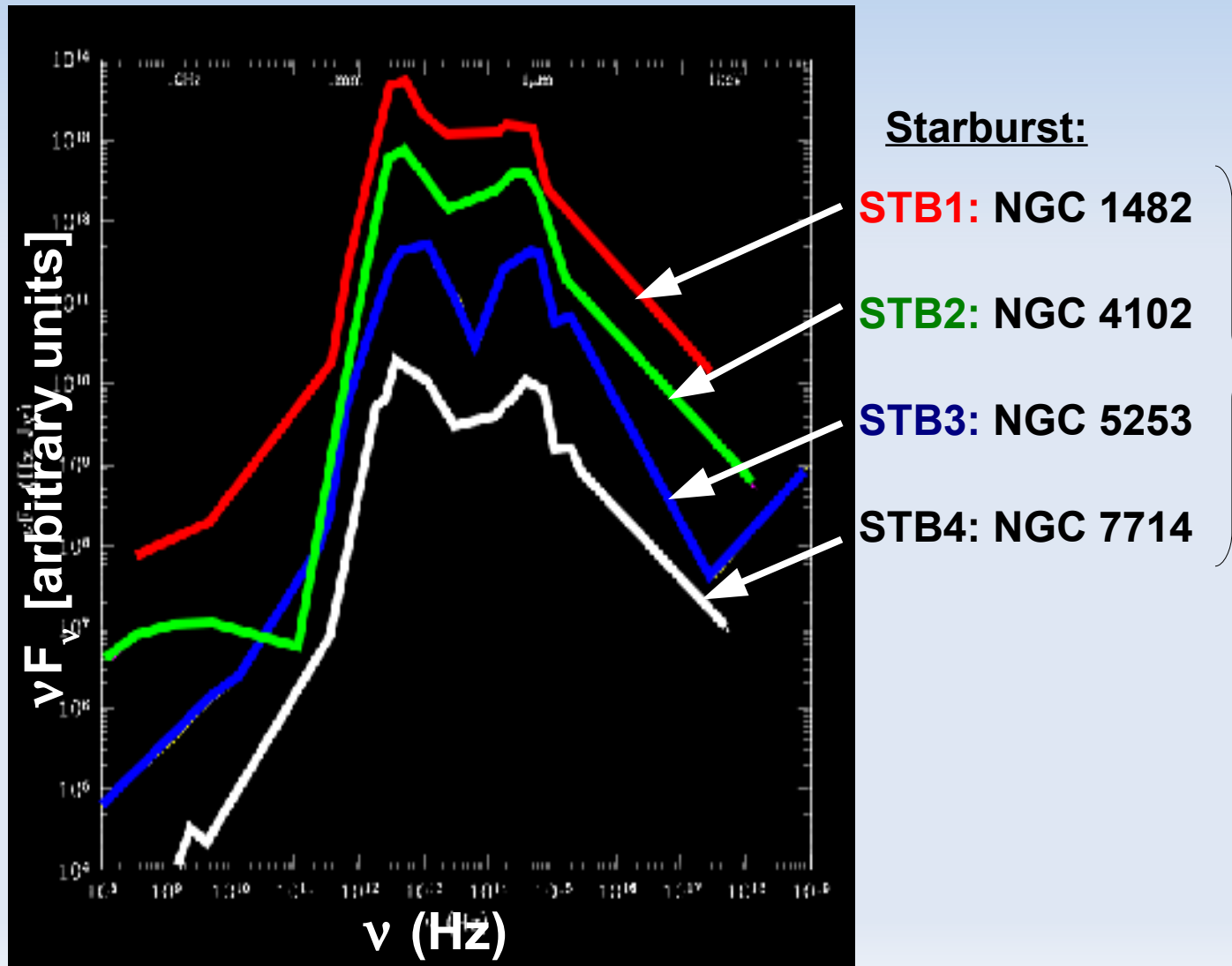


**Build and model the SED of each source  
in our sample (from radio to X-rays)**



# Templates

- Well observed SED of local STB and AGN

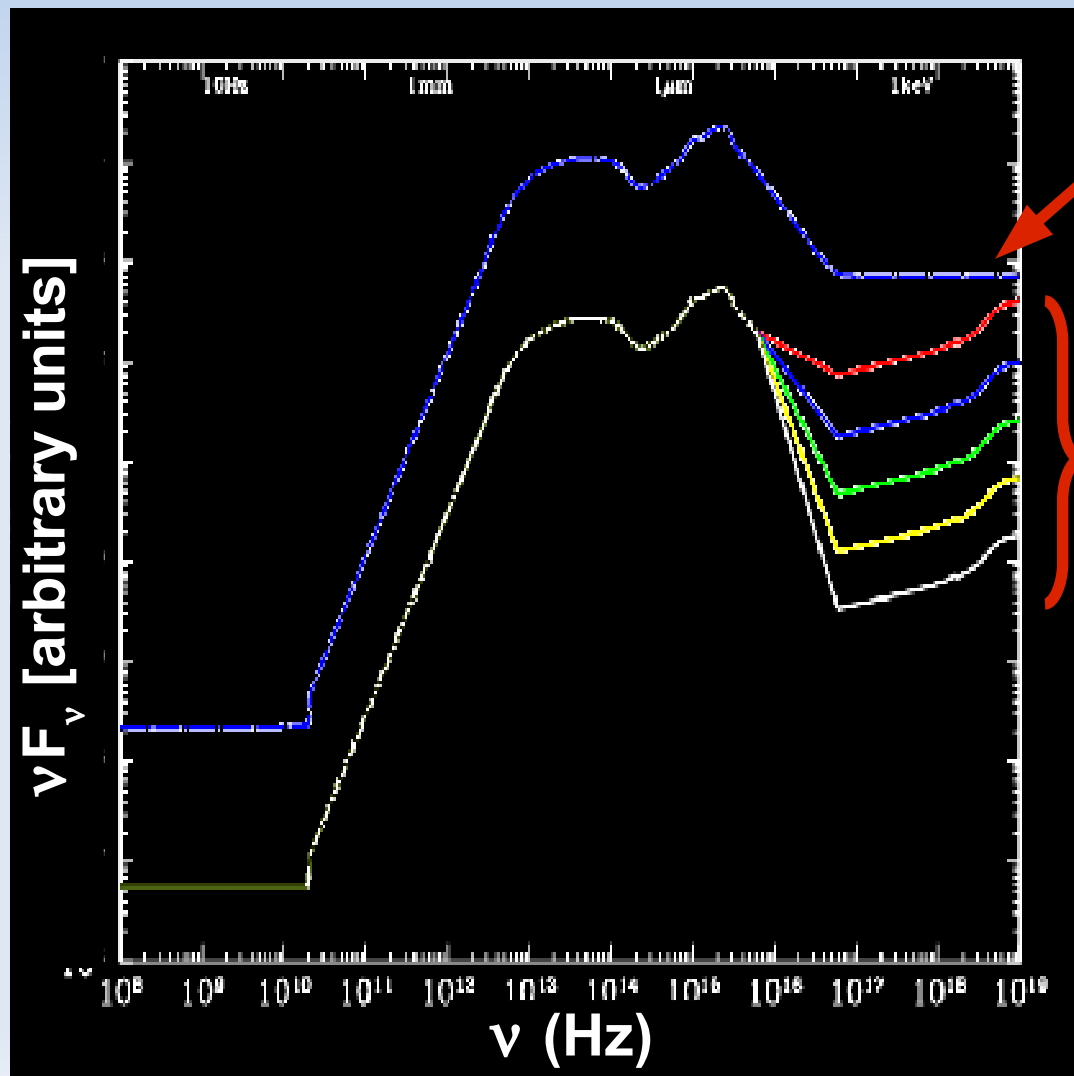


Different  
obscuration, width,  
intensity and peak  
wavelength



# Templates

- Well observed SED of local STB and AGN



### Type 1 RQ QSO mean SED:

Elvis et al. 1994:  $\log \nu < 12$

Richards et al. 2006:  $\log \nu > 12$

### RQ QSO luminosity-dependent SED:

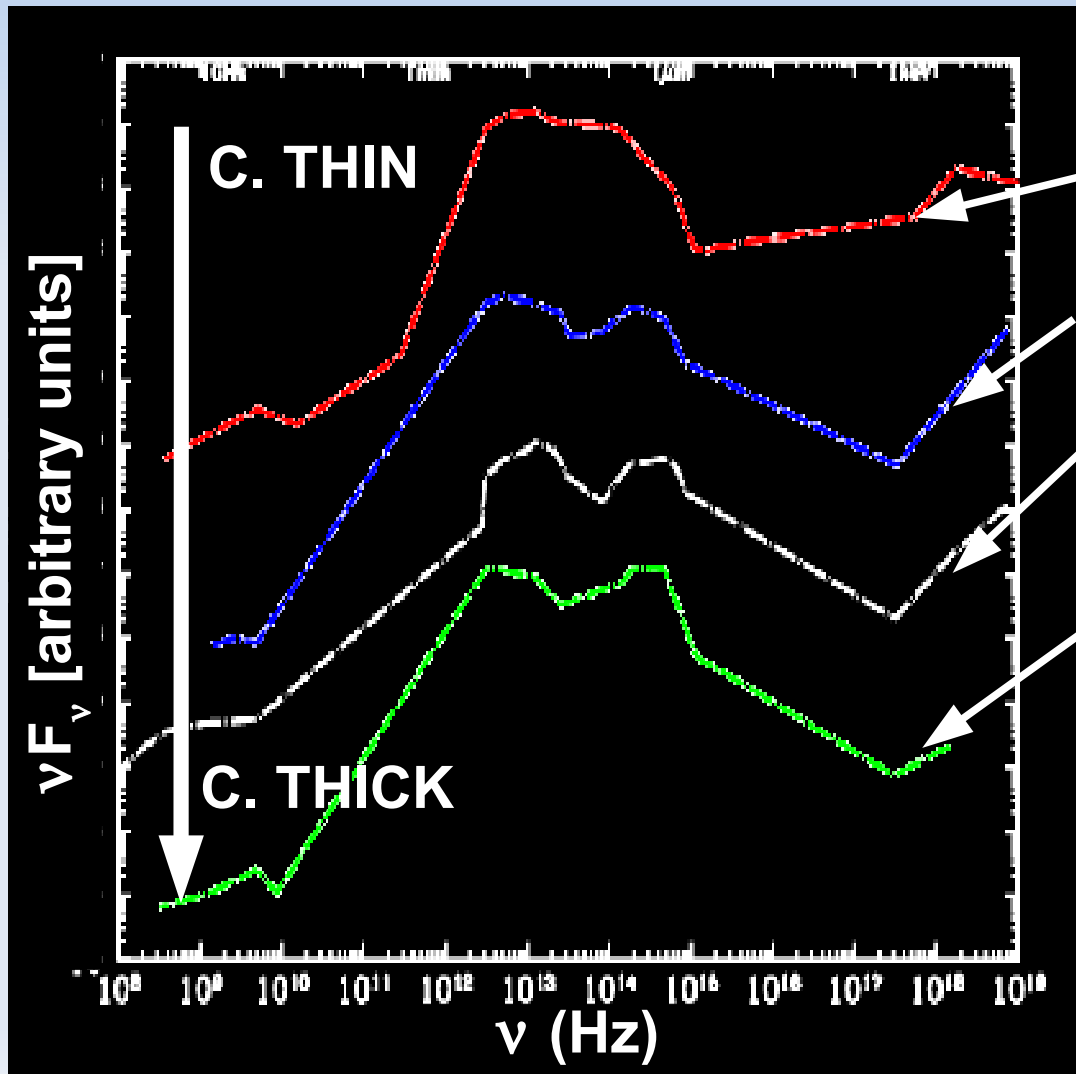
Hopkins, Richards & Hernquist 2007

$\alpha_{\text{ox}}$  increase with  $L_{\text{BOL}}$



# Templates

- Well observed SED of local STB and AGN



**AGN3: NGC 5506**  
( $N_H = 3 \times 10^{22} \text{ cm}^{-2}$ )

**AGN4: NGC 4507**  
( $N_H = 4 \times 10^{23} \text{ cm}^{-2}$ )

**AGN5: Mrk 3**  
( $N_H = 1 \times 10^{24} \text{ cm}^{-2}$ )

**AGN6: NGC 3393**  
( $N_H > 10^{25} \text{ cm}^{-2}$ )

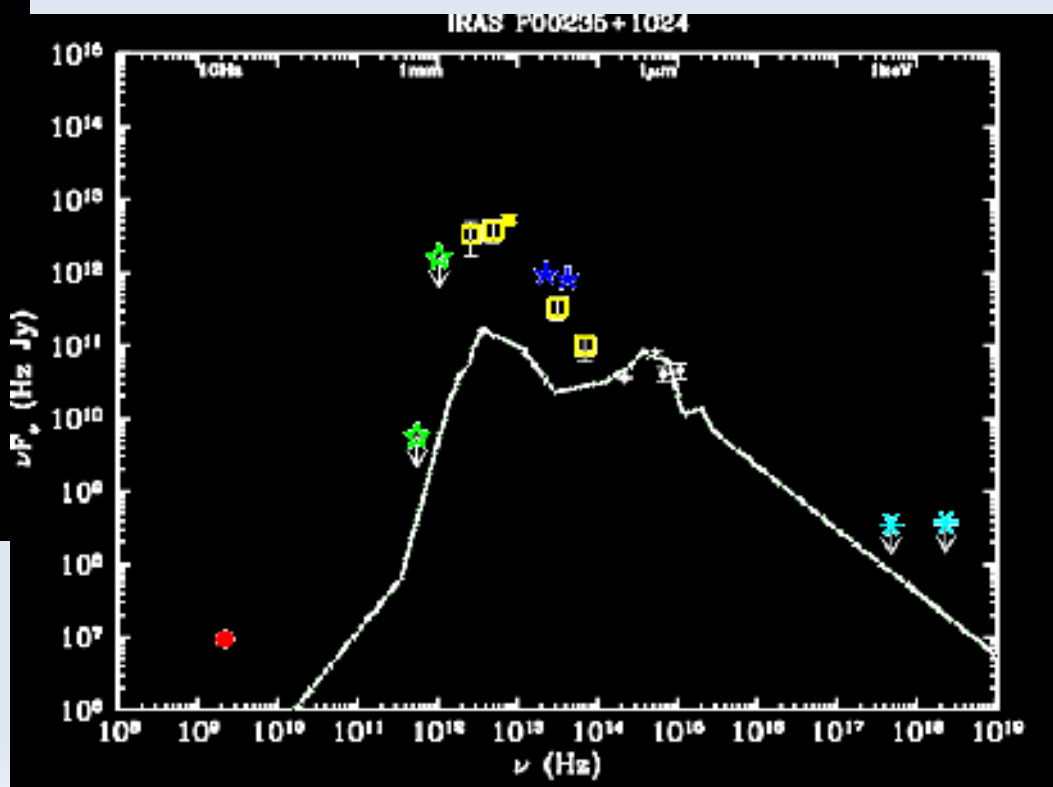
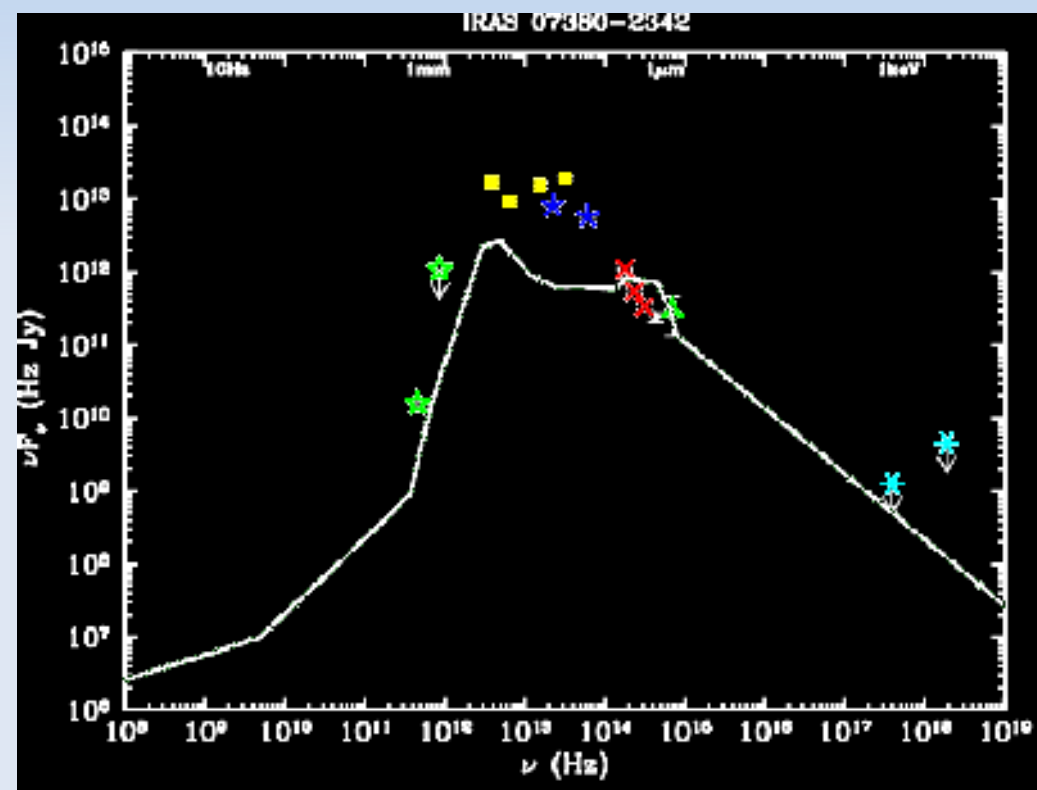
**Type 2 AGN**  
(different obscuration level)

From **Bianchi et al. 2006**  
Sy2 sample with  
**minimal starburst contribution**



# SEDs of HLIRGs

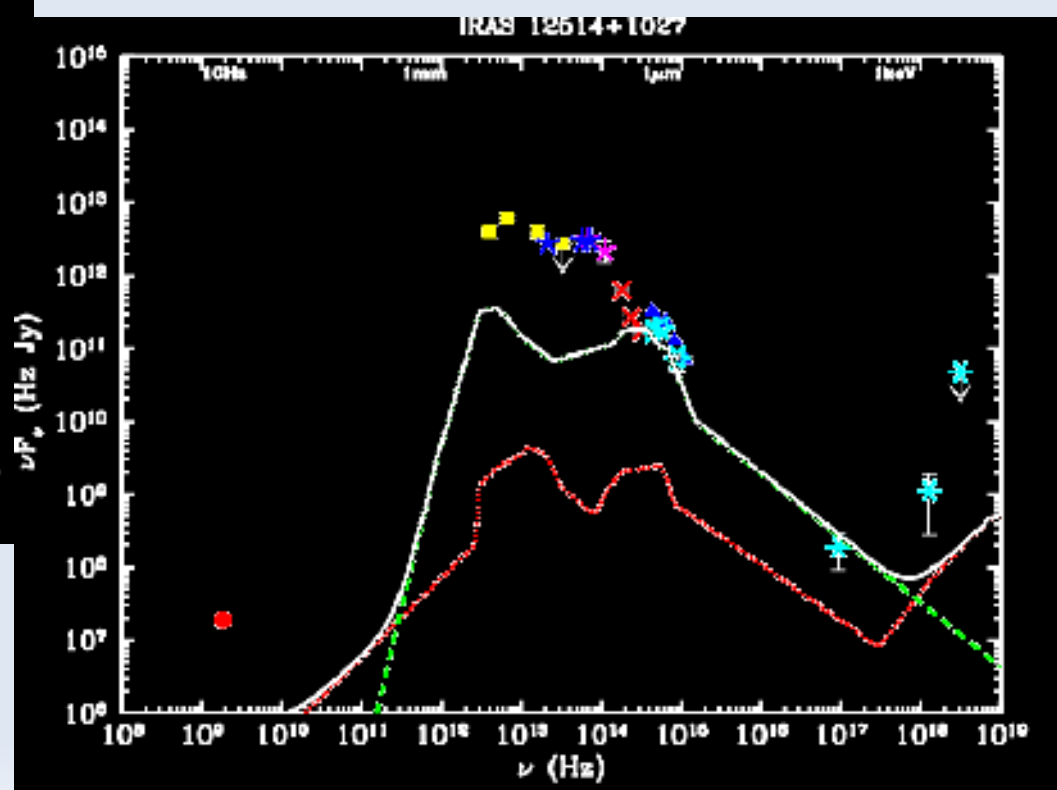
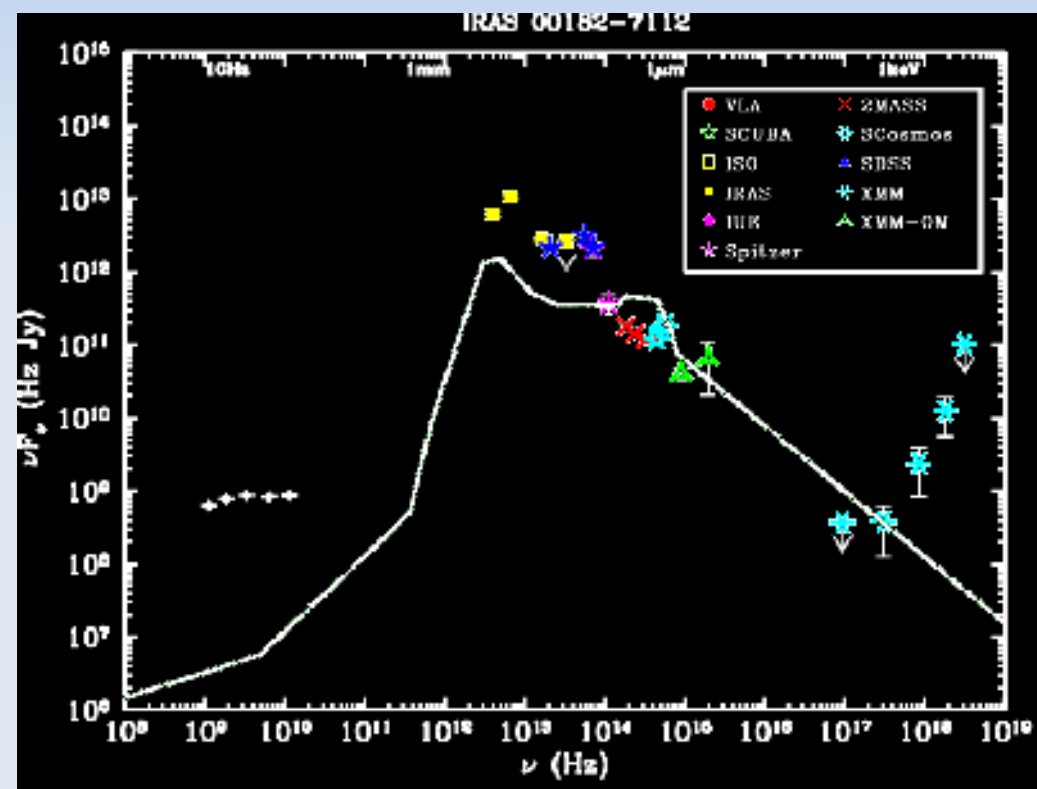
- Starburst (opt.)





# SEDs of HLIRGs

- Type 2 AGN sources (opt.)

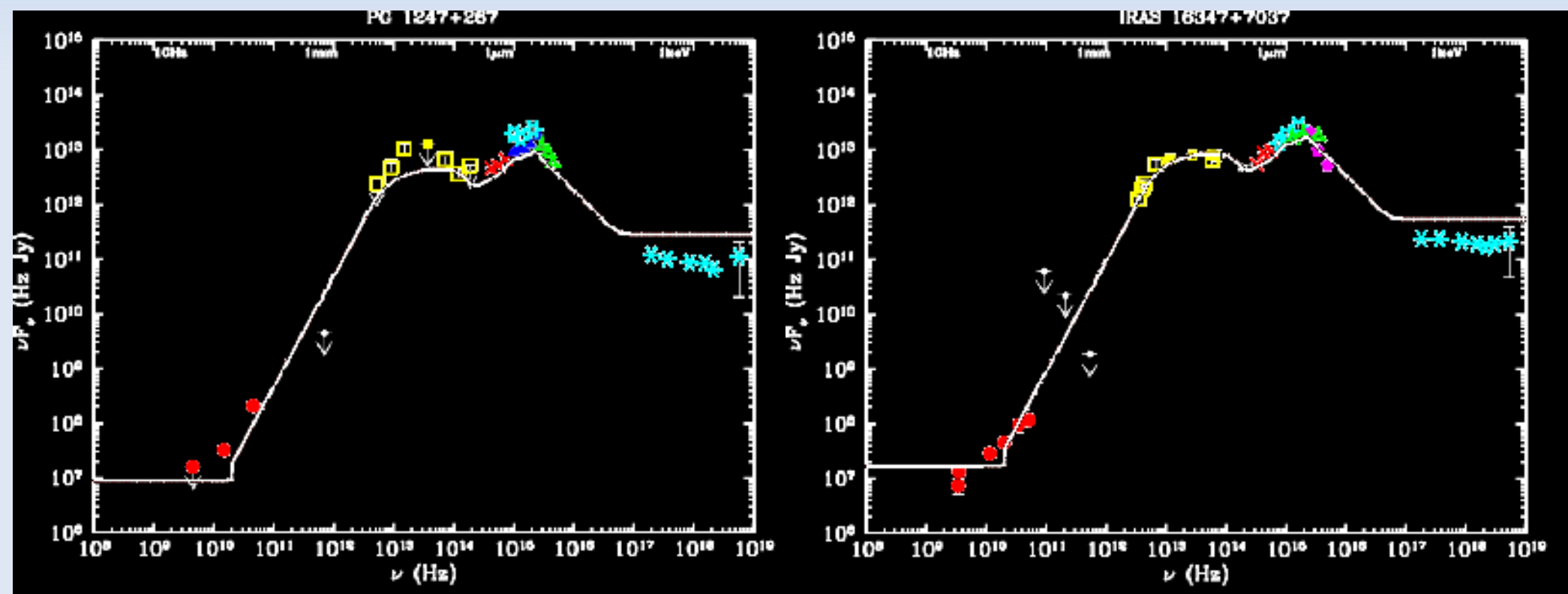




# SEDs of HLIRGs

- Type 1 AGN sources (opt.)

non-Luminosity-dependent SED

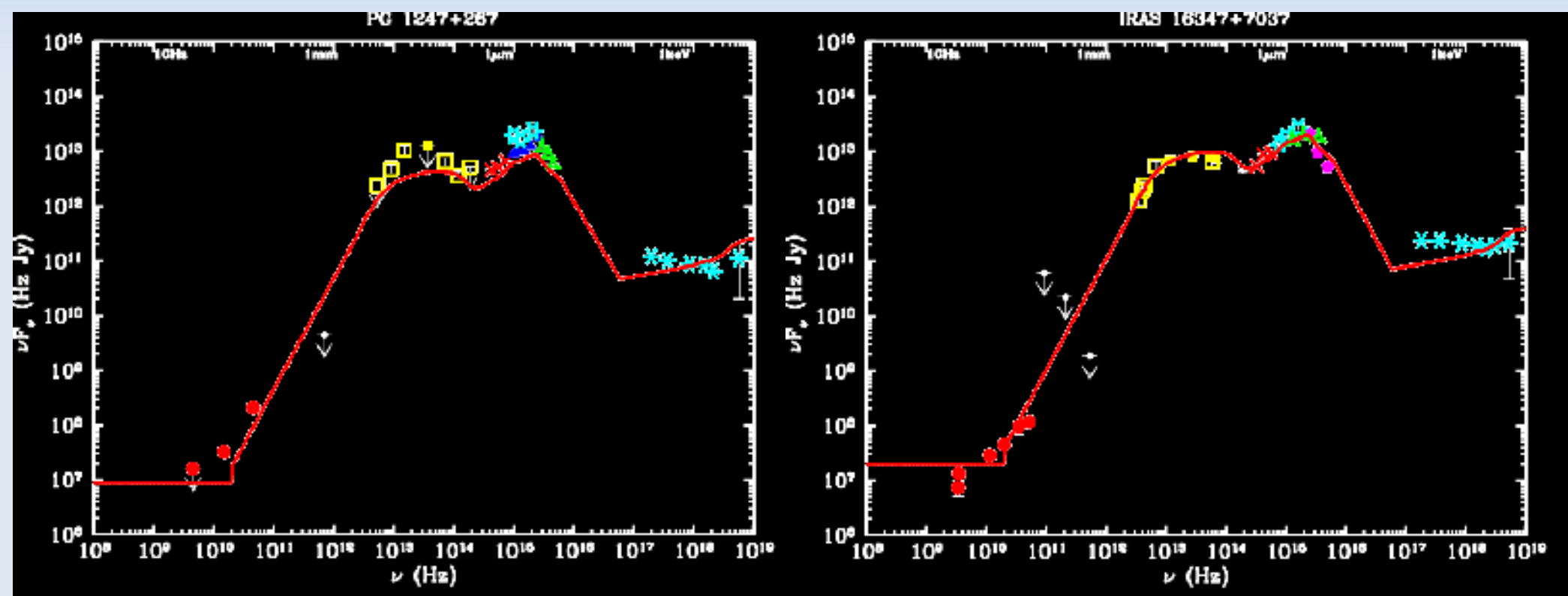




# SEDs of HLIRGs

- Type 1 AGN sources (opt.)

Luminosity-dependent SED

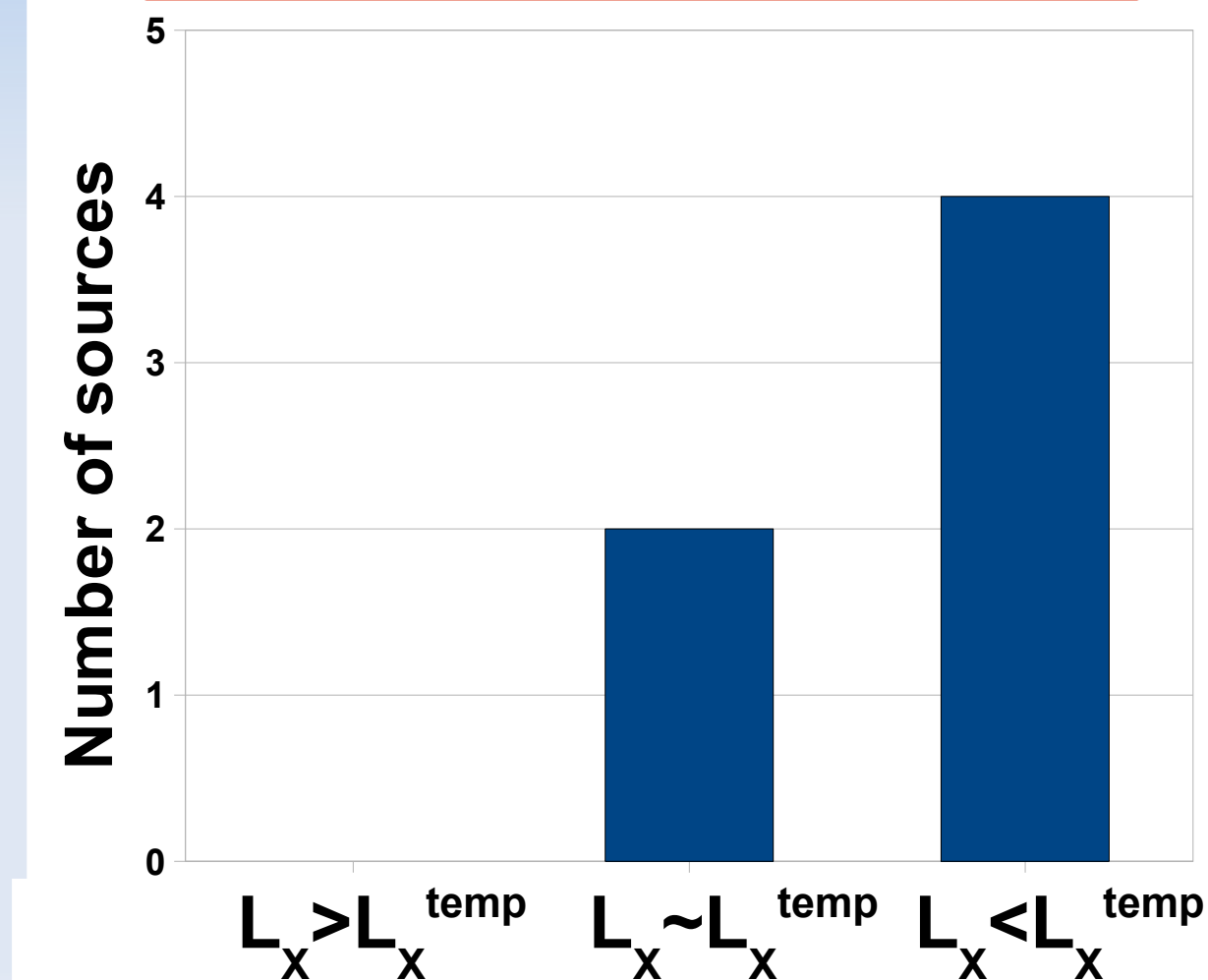




# SED of HLIRGs

- Type 1 AGN sources (opt.)

non-Luminosity-dependent SED

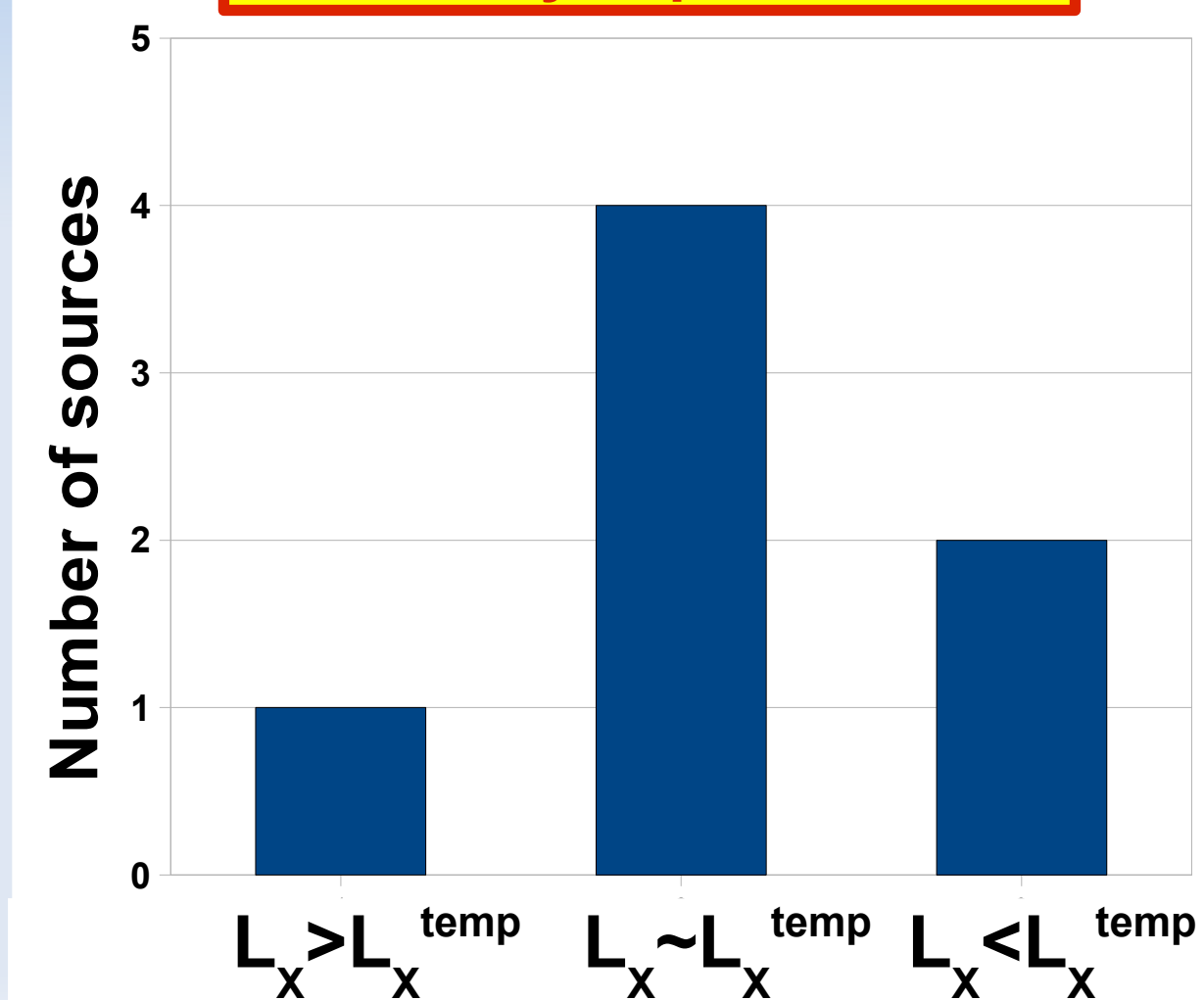




# SED of HLRGs

- Type 1 AGN sources (opt.)

Luminosity-dependent SED



# Fitting without X-ray data

| <b>Source</b>           | <b>Best fit</b> |             | <b><math>\log L_{BOL}</math></b> | <b>AGN / STB</b> | <b>CT?</b> |
|-------------------------|-----------------|-------------|----------------------------------|------------------|------------|
| <b>IRAS F00235+1024</b> | <b>AGN3</b>     |             | <b>46.0</b>                      | <b>1 / 0</b>     | <b>✓</b>   |
| <b>IRAS 07380-2342</b>  | <b>AGN3</b>     |             | <b>46.6</b>                      | <b>1 / 0</b>     | <b>X</b>   |
| <b>IRAS 00182-7112</b>  | <b>AGN3</b>     |             | <b>46.5</b>                      | <b>1 / 0</b>     | <b>✓</b>   |
| <b>IRAS 09104+4109</b>  | <b>AGN3</b>     | <b>STB4</b> | <b>47.0</b>                      | <b>0.9 / 0.1</b> | <b>✓</b>   |
| <b>IRAS 12514+1027</b>  | <b>AGN3</b>     | <b>STB4</b> | <b>46.4</b>                      | <b>0.9 / 0.1</b> | <b>✓</b>   |
| <b>IRAS F15307+3252</b> | <b>AGN1</b>     | <b>STB1</b> | <b>47.0</b>                      | <b>0.2 / 0.8</b> | <b>✓</b>   |
| <b>PG 1206+459</b>      | <b>AGN1</b>     |             | <b>48.4</b>                      | <b>1 / 0</b>     | <b>X</b>   |
| <b>PG 1247+267</b>      | <b>AGN1</b>     |             | <b>49.2</b>                      | <b>1 / 0</b>     | <b>X</b>   |
| <b>IRAS F12509+3122</b> | <b>AGN1</b>     |             | <b>47.4</b>                      | <b>1 / 0</b>     | <b>X</b>   |
| <b>IRAS 14026+4341</b>  | <b>AGN1</b>     | <b>STB4</b> | <b>46.8</b>                      | <b>0.3 / 0.7</b> | <b>X</b>   |
| <b>IRAS F14218+3845</b> | <b>AGN1</b>     |             | <b>47.0</b>                      | <b>1 / 0</b>     | <b>X</b>   |
| <b>IRAS 16347+7037</b>  | <b>AGN1</b>     |             | <b>48.9</b>                      | <b>1 / 0</b>     | <b>X</b>   |
| <b>IRAS 18216+6418</b>  | <b>AGN1</b>     | <b>STB1</b> | <b>47.4</b>                      | <b>0.8 / 0.2</b> | <b>X</b>   |

# Fitting with X-ray data

| Source           | Best fit | $\log L_{BOL}$ | AGN / STB | CT? |
|------------------|----------|----------------|-----------|-----|
| IRAS F00235+1024 | STB4     | 45.6           | 0 / 1     | ✓   |
| IRAS 07380-2342  | STB1     | 46.2           | 0 / 1     | ✗   |
| IRAS 00182-7112  | STB1     | 46.1           | 0 / 1     | ✓   |
| IRAS 09104+4109  | AGN3     | 46.9           | 0.6 / 0.4 | ✓   |
| IRAS 12514+1027  | AGN5     | 47.2           | 0.5 / 0.5 | ✓   |
| IRAS F15307+3252 | AGN5     | 47.0           | 0.8 / 0.2 | ✓   |
| PG 1206+459      | AGN1     | 48.4           | 1 / 0     | ✗   |
| PG 1247+267      | AGN1     | 49.2           | 1 / 0     | ✗   |
| IRAS F12509+3122 | AGN1     | 47.4           | 1 / 0     | ✗   |
| IRAS 14026+4341  | STB4     | 46.8           | 0 / 1     | ✗   |
| IRAS F14218+3845 | AGN1     | 47.0           | 1 / 0     | ✗   |
| IRAS 16347+7037  | AGN1     | 48.9           | 1 / 0     | ✗   |
| IRAS 18216+6418  | STB1     | 47.5           | 0.7 / 0.3 | ✗   |

Compton Thick

| Source           | Best fit |      | $\log L_{BOL}$ | AGN / STB | CT? |
|------------------|----------|------|----------------|-----------|-----|
| IRAS F00235+1024 |          | STB4 | 45.6           | 0 / 1     | ✓   |
| IRAS 07380-2342  |          | STB1 | 46.2           | 0 / 1     | ✗   |
| IRAS 00182-7112  |          | STB1 | 46.1           | 0 / 1     | ✓   |
| IRAS 09104+4109  | AGN3     | STB1 | 46.9           | 0.6 / 0.4 | ✓   |
| IRAS 12514+1027  | AGN5     | STB2 | 47.2           | 0.5 / 0.5 | ✓   |
| IRAS F15307+3252 | AGN5     | STB4 | 47.0           | 0.8 / 0.2 | ✓   |
| PG 1206+459      | AGN1     |      | 48.4           | 1 / 0     | ✗   |
| PG 1247+267      | AGN1     |      | 49.2           | 1 / 0     | ✗   |
| IRAS F12509+3122 | AGN1     |      | 47.4           | 1 / 0     | ✗   |
| IRAS 14026+4341  |          | STB4 | 46.8           | 0 / 1     | ✗   |
| IRAS F14218+3845 | AGN1     |      | 47.0           | 1 / 0     | ✗   |
| IRAS 16347+7037  | AGN1     |      | 48.9           | 1 / 0     | ✗   |
| IRAS 18216+6418  | AGN1     | STB1 | 47.5           | 0.7 / 0.3 | ✗   |

AGN only: 5 sources

| Source           | Best fit |      | $\log L_{BOL}$ | AGN / STB | CT? |
|------------------|----------|------|----------------|-----------|-----|
| IRAS F00235+1024 |          | STB4 | 45.6           | 0 / 1     | ✓   |
| IRAS 07380-2342  |          | STB1 | 46.2           | 0 / 1     | ✗   |
| IRAS 00182-7112  |          | STB1 | 46.1           | 0 / 1     | ✓   |
| IRAS 09104+4109  | AGN3     | STB1 | 46.9           | 0.6 / 0.4 | ✓   |
| IRAS 12514+1027  | AGN5     | STB2 | 47.2           | 0.5 / 0.5 | ✓   |
| IRAS F15307+3252 | AGN5     | STB4 | 47.0           | 0.8 / 0.2 | ✓   |
| PG 1206+459      | AGN1     |      | 48.4           | 1 / 0     | ✗   |
| PG 1247+267      | AGN1     |      | 49.2           | 1 / 0     | ✗   |
| IRAS F12509+3122 | AGN1     |      | 47.4           | 1 / 0     | ✗   |
| IRAS 14026+4341  |          | STB4 | 46.8           | 0 / 1     | ✗   |
| IRAS F14218+3845 | AGN1     |      | 47.0           | 1 / 0     | ✗   |
| IRAS 16347+7037  | AGN1     |      | 48.9           | 1 / 0     | ✗   |
| IRAS 18216+6418  | AGN1     | STB1 | 47.5           | 0.7 / 0.3 | ✗   |

SB only: 4 sources

| Source           | Best fit |      | $\log L_{BOL}$ | AGN / STB | CT? |
|------------------|----------|------|----------------|-----------|-----|
| IRAS F00235+1024 |          | STB4 | 45.6           | 0 / 1     | ✓   |
| IRAS 07380-2342  |          | STB1 | 46.2           | 0 / 1     | ✗   |
| IRAS 00182-7112  |          | STB1 | 46.1           | 0 / 1     | ✓   |
| IRAS 09104+4109  | AGN3     | STB1 | 46.9           | 0.6 / 0.4 | ✓   |
| IRAS 12514+1027  | AGN5     | STB2 | 47.2           | 0.5 / 0.5 | ✓   |
| IRAS F15307+3252 | AGN5     | STB4 | 47.0           | 0.8 / 0.2 | ✓   |
| PG 1206+459      | AGN1     |      | 48.4           | 1 / 0     | ✗   |
| PG 1247+267      | AGN1     |      | 49.2           | 1 / 0     | ✗   |
| IRAS F12509+3122 | AGN1     |      | 47.4           | 1 / 0     | ✗   |
| IRAS 14026+4341  |          | STB4 | 46.8           | 0 / 1     | ✗   |
| IRAS F14218+3845 | AGN1     |      | 47.0           | 1 / 0     | ✗   |
| IRAS 16347+7037  | AGN1     |      | 48.9           | 1 / 0     | ✗   |
| IRAS 18216+6418  | AGN1     | STB1 | 47.5           | 0.7 / 0.3 | ✗   |

Composite: 4 sources

| Source           | Best fit |      | $\log L_{BOL}$ | AGN / STB | CT? |
|------------------|----------|------|----------------|-----------|-----|
| IRAS F00235+1024 |          | STB4 | 45.6           | 0 / 1     | ✓   |
| IRAS 07380-2342  |          | STB1 | 46.2           | 0 / 1     | ✗   |
| IRAS 00182-7112  |          | STB1 | 46.1           | 0 / 1     | ✓   |
| IRAS 09104+4109  | AGN3     | STB1 | 46.9           | 0.6 / 0.4 | ✓   |
| IRAS 12514+1027  | AGN5     | STB2 | 47.2           | 0.5 / 0.5 | ✓   |
| IRAS F15307+3252 | AGN5     | STB4 | 47.0           | 0.8 / 0.2 | ✓   |
| PG 1206+459      | AGN1     |      | 48.4           | 1 / 0     | ✗   |
| PG 1247+267      | AGN1     |      | 49.2           | 1 / 0     | ✗   |
| IRAS F12509+3122 | AGN1     |      | 47.4           | 1 / 0     | ✗   |
| IRAS 14026+4341  |          | STB4 | 46.8           | 0 / 1     | ✗   |
| IRAS F14218+3845 | AGN1     |      | 47.0           | 1 / 0     | ✗   |
| IRAS 16347+7037  | AGN1     |      | 48.9           | 1 / 0     | ✗   |
| IRAS 18216+6418  | AGN1     | STB1 | 47.5           | 0.7 / 0.3 | ✗   |

| Source                                      | Best fit | $\log L_{BOL}$ | AGN / STB | CT? |
|---|----------|----------------|-----------|-----|
| IRAS F00235+1024                            | STB4     | 45.6           | 0 / 1     | ✓   |
| IRAS 07380-2342                             | STB1     | 46.2           | 0 / 1     | ✗   |
| IRAS 00182-7112                             | STB1     | 46.1           | 0 / 1     | ✓   |
| IRAS 09104+4109                             | AGN3     | 46.9           | 0.6 / 0.4 | ✓   |
| IRAS 12514+1027                             | AGN5     | 47.2           | 0.5 / 0.5 | ✓   |
| IRAS F15307+3252                            | AGN5     | 47.0           | 0.8 / 0.2 | ✓   |
| Bolometric output dominated by AGN emission |          |                |           |     |
| IRAS F12509+3122                            | AGN1     | 48.4           | 1 / 0     | ✗   |
| IRAS 14026+4341                             |          | 49.2           | 1 / 0     | ✗   |
| IRAS F14218+3845                            | AGN1     | 47.4           | 1 / 0     | ✗   |
| IRAS 16347+7037                             | AGN1     | 46.8           | 0 / 1     | ✗   |
| IRAS 18216+6418                             | AGN1     | 47.0           | 1 / 0     | ✗   |
|   | STB4     | 48.9           | 1 / 0     | ✗   |
|   |          | 47.5           | 0.7 / 0.3 | ✗   |



# Conclusions

- XMM-Newton-selected sample of **13 HLIRGs**:
  - 10/13 detected and **AGN-dominated in X-rays**:
  - Under luminous in X-rays with respect to mean SED of local QSO
- Modelling multi- $\lambda$  SED (from radio to X-rays):
  - SED fitting **consistent with the optical classification**
  - **9/13 need an AGN component**:
    - 5 pure AGN, 4 composite
    - STB templates preferred: NGC 1482 (**aged bursts**)
  - **AGN component dominates the bolometric output**
- **X-ray data are mandatory** for an accurate estimation of the relative AGN / STB contribution
- SED of **type 1 AGN** are consistent with a **luminosity dependent SED**